MARCH 1995 ECN-C--95-001

REALISATION AND FIELD TEST OF A SOLAR POWERED DEEP WELL PISTON PUMP

N.J.C.M. VAN DER BORG
J. TEN THIJE O.G. BOONKKAMP*

* UNIVERSITY OF TECHNOLOGY, FACULTY OF PHYSICS, LABORATORY OF FLUID DYNAMICS
HEAT TRANSFER, BUILDING W&S, P.O. BOX 513, 5600 MB EINDHOVEN

	Name	Signature	Date
Checked	**W.J. Stam**		29/11/95
Approved	**W.J. Stam**		28/3/95
Authorized	**H.J.M. Beurskens**		28/3/95

This work was part of the project "PV-pump system" funded by the EU (JOULE progamme, contract JOU2-CT92-0181) and by the Netherlands Ministry of Economic Affairs ("Doelsubsidieprogramma").

The main contractor of the JOU2-CT92-0181 project was the EUREC Agency. The technical coordination has been done by WIP, München.

ECN project number 4480-01.

CONTENTS

List of Symbols:

a,b,c,d,e,R	Coefficients (page 7)	
A_p	Piston area	($m^{2)}$
E	Elasticity modulus	(Pa)
g	Gravity constant	(m/s^2)
h	Lifting head	(m)
I_{sc}	Short circuit current	(A)
I	Current	(A)
n	Rotational speed	(rpm)
$P_{el.}$	Electric power	(W)
$P_{el,av.}$	1 minute averaged $P_{el.}$	(W)
$P_{mech.}$	Mechanical power	(W)
s	Piston stroke	(m)
T	Torque	(Nm)
U_{oc}	Open circuit voltage	(V)
V	Voltage	(V)
ε_{tg}	Tangential strain	(-)
ε_{ax}	Axial strain	(-)
ϕ	Flow	(m^3/s)
$\phi_{av.}$	1 minute averaged ϕ	(m^3/s)
η_{vol}	Volumetric efficiency	(%)
η_{sub}	Subsystem efficiency	(%)
ρ	Density of water	(kg/m^3)
ν	Poissons ratio	(-)
σ_{tg}	Tangential stress	(Pa)
σ_{ax}	Axial stress	(Pa)

1. INTRODUCTION

In the frame of the CEC-funded project "Development of a high efficiency PV driven displacement pump system for application in rural areas" (JOU2-CT92-0181), ECN and TUE have developed a PV driven piston pump for deep well water pumping. The aim of the work was to design, build and test the pump system with the purpose of checking the viability of the chosen concept.

The principle of the pump system has been initiated by the TUE. Basically the pump system consists of a PV-array, an electric motor and a slightly modified normal handpump. The pump system contains no electronic equipment for the purpose of DC/DC matching, maximum power point tracking or power boosting. These features have been facilitated using a special piston valve: the TUE-matching valve.

A PV piston pump equipped with the TUE matching valve has been realised in Petten. A short description of the pump system is given in chapter 2. For the purpose of the orientating field test the pump has been installed in a bore hole with adjustable water table up to 50 meter below ground level on the ECN test station. The solar arrays have been simulated by a power supply with comparable characteristics as a solar array. With these facilities a number of tests have been performed. After some initial tests small modifications have been made to the pump system. The modifications are briefly described in chapter 2. The procedures of testing and the data treatment are given in chapter 3. The results of two "final" tests are also presented in chapter 3. Conclusions of these tests have been formulated in chapter 4. After the orientating field test the pump system will be tested in the laboratories of Genec in France.

The results of the field test in Petten have been used for the parameter fitting of the dynamical model of the pump system, developed by TUE (ref. [2]).

2. PV PUMP SYSTEM

The pump system is depicted in figure 1. The following items can be distinguished.

Solar panel
For the purpose of the experiments the solar panel has been simulated by a DC power supply with a I-V characteristic comparable to a real PV array. The characteristic is given in figure 2. The open circuit voltage and the short circuit current of the power supply can be set manually.

Motor
The electric motor has been manufactured by CREUSEN, the Netherlands. It is a permanent magnet direct current motor of the model 90M-4GPVEK-83. The nominal output power is 330 W at 80 Vdc and 5 A. The price was Dfl 853.--.
The characteristics of the motor have been measured in the laboratory of the TUE using a mechanical load with adjustable torque. During the experiments the torque and the rotational speed of the motor have been measured at various combinations of voltage (up to 100 V) and current (up to 4 A) of the motor. The results have been used to determine the coefficients of the following motor model.
$n = a.V - R.I - b$ and $T = -c.V + d.I - e$

with
- n = rotational speed of the motor (rpm)
- V = voltage on the motor (V)
- I = current through the motor (A)
- T = torque of the motor (Nm)

R, a, b, c, d = coefficients

The determined values of the coeffients are:
- R = 23.41 rpm/A
- a = 9.435 rpm/V
- b = 12.9 rpm
- c = $5.839.10^{-4}$ Nm/V
- d = 1.003 Nm/A

Transmission
The transmission from the motor to the flywheel has been facilitated by a pulley on the motor, a normal driving belt and the (unmodified) flywheel of the handpump. Initially an industrial driving belt was used with a width of 100 mm. This however caused an unnecessary high power consumption. Hereafter an ad hoc manufactured driving belt was used for some experiments. During these experiments sometimes slip between the belt and the pulley has been observed. Later it was decided to use a strip (width 15 mm) of the original belt. As an extra precaution to prevent slip the pulley has been covered with sand paper for the duration of the experiments. The diameter of the motor pulley and the pump flywheel was 125 mm (excluding the sand paper) and 1500 mm respectively. As a consequence the nominal transmission ratio was 12.

Handpump
A commercial available handpump has been used to complete the system. The handpump of the type VOLANTA has been manufactured by Jansen Venneboer B.V., The Netherlands. A copy from the brochure of the handpump is given in figure 3. The price of the complete handpump, including the pumprod and rising main for a pumping depth of 25 meter, including a pulley for the electric motor, including a driving belt and including the costs of transportation to Petten was Dfl. 4199.--.

The piston of the handpump has been replaced by a piston and a matching valve, both designed and manufactured by the TUE. A sketch of the piston and valve, made by the TUE, is given in figure 4. A photograph of the piston, matching valve, pump cylinder and foot valve is given in on page 23. The estimated production costs of these parts are equal to the production costs of the replaced Volanta-piston.

During initial experiments it was observed that the gland around the upper part of the pump rod caused much friction. Therefore the original gland has been replaced by a leather cup. When no additional lifting head is applied above ground level a negligible amount of water is leaking out of this cup. Experiments showed that this leakage is stopped completely for an additional lifting head (6 - 7 m) above ground level.

At low rotational speed, the TUE-matching valve intentionally does not close, due to its buoyance. This enables the pump system to accumulate energy for a pump stroke at a predicted rotational speed. In order to minimize the variations of the rotational speed, important for proper matching, the mass moment of inertia of the flywheel has been increased using additional lead masses. The estimated mass moment of inertia of the unmodified flywheel was 17 $kg.m^2$. Including the additional masses the estimated mass moment of inertia was 21 $kg.m^2$.

Rising main
The rising main is made of PVC and has an internal diameter of 70 mm and external diameter of 80 mm. The tubes have a length of 2.85 meter and are connected to each other by glued sockets.

To facilitate the determination of the mechanical stresses by measuring strain data of the rising main during the planned field test the values of the elasticity modulus and Poisson's ration have been measured in the laboratory of ECN. This has been done using a cylindrical vessel made of a part of the rising main. The internal pressure in this vessel has been set at various values and the corresponding axial and tangential stresses in the cylindrical wall of the vessel have been measured. Using the pressure values and the dimensions of the vessel the stresses have been calculated and the corresponding strains have been determined.

0 Elasticity modulus: 3.12 GPa;
0 Poisson's ration: 0.40

3. EXPERIMENTS

3.1 Measured quantities

Experiments have been performed at a number of simulated stationary insolation vallues. At each simulated insolation the following quantities have been measured during one minute.

* DC voltage of the power supply.
* DC current through the motor.
* RPM of the motor.
* Position of the piston and from this the rpm of the pump.
* Water flow.
* Force in the pump rod above the gland.
* Axial strain in the lower part of the rising main.
* Tangential strain in the lower part of the rising main.

These quantities have been measured by a PC with a sampling rate of 32 Hz per channel. Furthermore the settings of the short circuit current and the open circuit voltage have been measured at the start of each experiment. The water table has been measured using a rope and an ullage.

3.2 Derived quantities

From the measured quantities the following quantities have been derived:

* Electric power.
  The electric power delivered by the power supply is determined by multiplying the voltage and current at each sample. The power loss in the cable between power supply and motor is maximum 2 percent and has been neglected.
  $P_{el} = V \cdot I$.
* RPM of the pump.
  The number of pump strokes per minute has been determined for each experiment by counting the number of cycles obtained from the position signal.
* Mechanical power.
  The mechanical power on the shaft of the motor has been calculated per sample from the measured rotational speed of the motor and the torque on the shaft.
  $P_{mech.} = T \cdot 2\pi \cdot n/60$.
  The torque has not been measured directly. Its value has been calculated for each sample by using the measured voltage and current and the relation between torque, voltage and current.
  $T = -c \cdot V + d \cdot I - e$.
  The coefficients c, d and e are given in chapter 2.
* Motor efficiency.
  The motor efficiency has been obtained per sample from the electric power and the mechanical power.
  $\eta_{motor} = (P_{mech.}/V \cdot I) \cdot 100\%$.

* Tracking efficiency.
  The efficiency of the maximum power point tracking has been calculated per sample by dividing the electric power from the simulated array by the power at the maximum power point at the simulated insolation. This maximum power is equal to the open circuit voltage multiplied by the short circuit current and by the fill factor of the simulated PV array. The applied fill factor was 0.70.
  $\eta_{tracking} = (I \cdot V / 0.7 \cdot U_{oc} \cdot I_{sc}) \cdot 100\%$.
* Subsystem efficiency.
  The efficiency of the subsystem from the electric power to the net hydraulic power has been calculated using the one minute averaged value of the flow ($\phi_{av.}$), the lifting head and the one-minute averaged electric power ($P_{el.,av.}$).
  $\eta_{sub} = (\phi_{av.} \cdot \rho \cdot g \cdot h / P_{el.,av.}) \cdot 100\%$.
* Volumetric efficiency.
  The volumetric efficiency of the pump has been calculated from the one-minute averaged value of the flow, the number of pump strokes per minute and the piston diameter and stroke length. The stroke length has not been corrected for the cyclic changes in the length of the pump rod and the rising main.
  $\eta_{vol} = (\phi_{av.} \cdot 60 / n_{pump} \cdot A_p \cdot s) \cdot 100\%$.
* Range of the pumprod force.
  The range of the pumprod force has been determined per minute as the difference between the highest and the lowest measured value during that minute.
* Range of the stress in the rising main.
  The stress in the lower part of the rising main has been determined in the two principal directions (axial and tangential) from the measured tangential and axial strains and the elasticity modulus and Poisson's ratio of the rising main.
  $\sigma_{tg} = E(\varepsilon_{tg} + \nu \cdot \varepsilon_{ax}) / (1 - \nu^2)$.
  $\sigma_{ax} = E(\varepsilon_{ax} + \nu \cdot \varepsilon_{tg}) / (1 - \nu^2)$.
  The range of the axial stress has been determined per minute as the difference between the highest and the lowest measured value during that minute. For the tangential stress the same has been done.

3.3 Results

3.3.1 Lifting head 25.5 meter

A series of experiments has carried out for a water lifting head of 25.5 m. The water table was 24.5 m under ground level and the water sprout was 1 m above ground level. As a consequence the pressure inside the system at the gland was almost atmospheric. A negligible amount of water was leaking from the gland. The lifting height of the TUE matching valve was 5.35 mm. The piston was a few meter under the water table. The ad hoc manufactured transmission belt was extremely flexible but it caused sometimes slip.
The simulated PV array was one string of four RSM 45 modules in series. The nominal peak power per module is 45 W, the open circuit voltage is 21 V and the short circuit current at 1000 W/m² is 3.1 A.
Tests have been performed during quasi-static conditions during periods of one-minute during which the simulated insolation was kept constant (one

minute per simulated insolation). As examples some measured and derived quantities are presented as a function of time in the figures 5.1. through 5.8. The one-minute averaged values of the relevant measured and derived quantities are presented in table 1. In this table only the ranges in the tangential stress in the rising main has been presented because during all experiments the ranges in tangential stress was higher than the variations in axial stress.

3.3.2 Lifting head 44.6 meter

A series of experiments has been carried out with a lifting head of 44.2 meter. However after dismantling the pump system it was noticed that during these experiments the holes in the leather cup had not been completely in line with the holes in the piston (see figure 4). As a consequence the hydraulic energy losses must have been higher than in the normal situation. Furthermore a mistake had been made with the measurement signal of the pumprod force. Hereafter the measurements have been repeated with the holes in line and with a water lifting head of 44.6 m. The water table was 37.9 m under ground level and the water sprout was 6.7 m above ground level. As a consequence the pressure inside the system at the gland was about 66 kPa. No water was leaking from the gland. The lift height of the TUE matching valve was 6.8 mm. The piston was a few meter under the water table. The transmission belt has been cut from a normal industrial transmission belt. Its width was 15 mm and the belt was very flexible. To prevent slipping the motor pulley was covered with sand paper for the duration of the experiment. During the test the driving belt had the tendency to "climb" on the edge of the motor pulley. Therefore the transmission ratio was during the experiments between 11 and 12.

The simulated PV array consisted of two parallel strings of four RSM 45 modules in series. This means that the installed power was twice as high as during the experiments with a head of 25.5 m and that the open circuit voltage of both series of experiments was the same.
Tests have been performed during quasi-static conditions during periods of one-minute during which the simulated insolation was kept constant. As examples, some measured and derived quantities are presented as a function of time in the figures 6.1. through 6.8. The one-minute averaged values of the relevant measured and derived quantities are presented in table 2. In this table only the ranges of the tangential stress in the rising main has been presented because during all experiments the ranges of the tangential stress was higher than the variations in axial stress.

3.3.3 Transmission losses

For the estimation of the energy losses in the transmission experiments have been performed with a disconnected pumprod. The rotational speed of the motor has been set on various stationary values by adjusting the voltage of the power supply. The power delivered by the power supply is consumed by the motor, the transmission belt and the bearings of the flywheel. The measured electric power as a function of the motor rotational speed is given in figure 7 for the following transmission belts:
* industrial transmission belt;
* ad hoc transmission belt;

* no transmission belt.

In the case of no transmission belt no power is consumed by the belt and the flywheel bearings.

3.4 Discussion of the results

The time series of the measured and derived quantities (of which some examples have been given in the figures 5 and 6) can be used to gain a better understanding of the dynamic behaviour of the total system. The time series will not be discussed further in this document.

Using the tables 1 and 2, the figures 8, 9 and 10 have been made, showing the MPP-tracking efficiency, the subsystem efficiency and the water yield as a function of the insolation. The most relevant quantities in the tables are discussed below.

* Motor efficiency.
  The motor efficiency has values around 75%. At very low insolation values the efficiency drops.
* Tracking efficiency.
  The efficiency of the maximum power point tracking facilitated by the nature of the TUE matching valve varies between about 70% and 95% for the significant insolation values.
* Subsystem efficiency.
  The efficiency of the subsystem at an insolation of about 800 W/m^2 was 46% for the experiments with a head of 25.5 m and 42% for the experiments with a head of 44.6 m. The differences between these experiments were, apart from the lifting head, also the pressure on the gland and the type of transmission belt. As can be seen in figure 7 a significant part of the energy losses is introduced by the transmission.
* Pumprod forces.
  The observed range in the pumprod forces during the one-minute periods never exceeded 2.1 kN. The observed variations in pumprod force correspond to ranges in the mechanical stress in the pumprod of less than 42 MPa. This value is below the design fatigue strength for stainless steel rod of a handpump of 50 MPa (see appendix A, extracted from ref. 1, page IV-2). Since the measured ranges are rather close to the design fatigue strength the fatigue damage for a lifetime of 20 years has been calculated (see appendix B) using a safety factor of 2. This resulted in a SRF (Stress Reserve Factor) of 2.7 which means that the stresses are a factor 2.7 lower than the safe limits.
* Stress in rising main.
  The observed range of the stress in the rising main in tangential direction was always higher than in axial direction. The observed range in tangential direction during the experiments never exceeded 3 MPa. This value is below the design fatigue strength for a PVC rising main of a handpump of 6 MPa (see appendix A, extracted from ref. 1, page IV-3).

4. CONCLUSIONS

A PV driven piston pump, equipped with the TUE-matching valve, has been built. From the orientating field test the following conclusions can be drawn.

* The total pump system excluding the PV-array and excluding the bore hole has been realised for a total price of about Dfl. 5,000.-- (approx. 2,400 ECU).
* The pump system is able to pump water from a depth of 25 m (installed power 180 Wp) and from a depth of 45 m (installed power 360 Wp) with subsystem efficiencies above 40% for the significant insolation values.
* The maximum power point tracking efficiency is between 70 and 95% for the significant insolation range, which shows that the concept of the TUE-matching valve works.
* The dynamic loads in the system are below the design fatigue strengths.
* The total efficiency of the system can be improved by optimizing the gland, the electric motor and the transmission belt.

5. TABLES

Table 1 Results of the measurements with a lifting head of 25.5 m; installed solar power: 180 Wp

Driving belt: ad hoc manufactured.

Experiment code →		ZOPO 30	ZOPO 31	ZOPO 32	ZOPO 33	ZOPO 34	ZOPO 35
Simulated insolation	(w/m^2)	1000	806	645	484	323	225
Short circuit current	(A)	3.1	2.5	2.0	1.5	1.0	0.7
Open circuit voltage	(V)	84	84	84	84	84	84
Voltage	(V)	77.1	70.3	56.0	49.0	46.1	41.7
Electric power	(W)	158	139	94.2	64.0	37.3	24.2
Motor speed	(rpm)	640	578	454	400	387	353
Pump speed	(rpm)	49.7	46.0	36.0	33.5	32.7	30.0
Flow	(l/min)	17.20	15.25	9.15	5.53	1.49	0.0
Mechanical power	(W)	120	105	68.7	44.7	23.2	12.8
Motor efficiency	(%)	76.0	75.5	73.0	69.9	62.3	52.9
Tracking efficiency	(%)	86.5	94.7	80.1	72.5	63.4	58.7
Subsystem efficiency	(%)	45.5	45.9	40.5	36.0	16.7	0.0
Volumetric efficiency	(%)	92.8	88.9	68.1	44.2	12.2	0.0
Range pumprod force	(N)	1250	1180	1260	1270	1210	-
Range tangential stress	(kPa)	1500	1600	1900	1550	1400	-
n_{motor}/n_{pump}	(-)	12.9*)	12.6*)	12.6*)	11.9	11.8	11.8
*) slip in driving belt observed.							

Table 2 Results of the measurements with a lifting head of 44.6 m; installed solar power 360 Wp

Driving belt: industrial.

Experiment code →		ZO40 10	ZO40 11	ZO40 12	ZO40 13	ZO40 14	ZO40 15
Simulated insolation	(w/m^2)	1000	806	645	484	323	161
Short circuit current	(A)	6.2	5.0	4.0	3.0	2.0	1.0
Open circuit voltage	(V)	84	84	84	84	84	84
Voltage	(V)	79.5	76.8	64.2	55.5	48.5	9.2
Electric power	(W)	295	276	221	148	87.5	8.9
Motor speed	(rpm)	610	589	478	419	378	47
Pump speed	(rpm)	54.7	53.0	43.0	37.5	34.0	4.0
Flow	(l/min)	17.01	15.73	11.37	6.47	2.74	0.0
Mechanical power	(W)	223	206	160	106	62	3.7
Motor efficiency	(%)	75.0	74.8	72.5	71.9	70.6	42.1
Tracking efficiency	(%)	81.9	94.0	94.1	83.7	74.4	15.0
Subsystem efficiency	(%)	41.5	41.5	37.5	31.9	22.8	0.0
Volumetric efficiency	(%)	83.4	80.0	70.9	46.2	21.6	0.0
Range pumprod force	(N)	1915	1889	2007	2090	2056	262
Range tangential stress	(kPa)	2229	1857	2615	2623	2235	36
n_{motor}/n_{pump}	(-)	11.2	11.1	11.1	11.2	11.1	(11.8)

6. REFERENCES

[1] Jos Besselink, Jacques Grupa and Paul Smulders: "Behaviour of deepwell handpumps with PVC rising mains"; publisher: APP b.v. Ellecom, The Netherlands, ISBN 90-6618-544-9.

[2] J. ten Thije o.g. Boonkkamp: "Analysis of a solar powered piston pump tested at ECN, Petten; Report R1366D, Laboratory of fluid dynamic and heat transfer, Faculty of Physics, TUE.

7. FIGURES

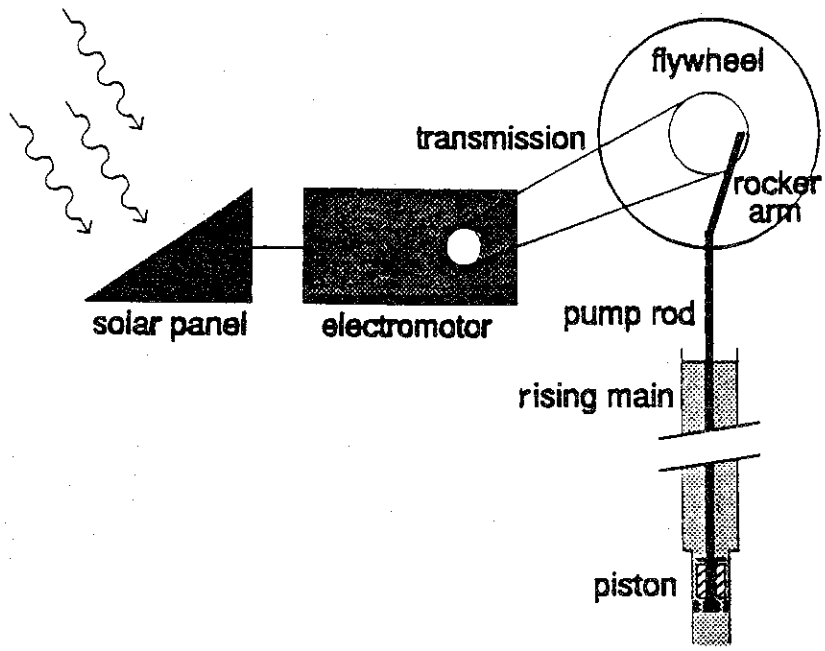

Figure 1 The components of the solar pump.

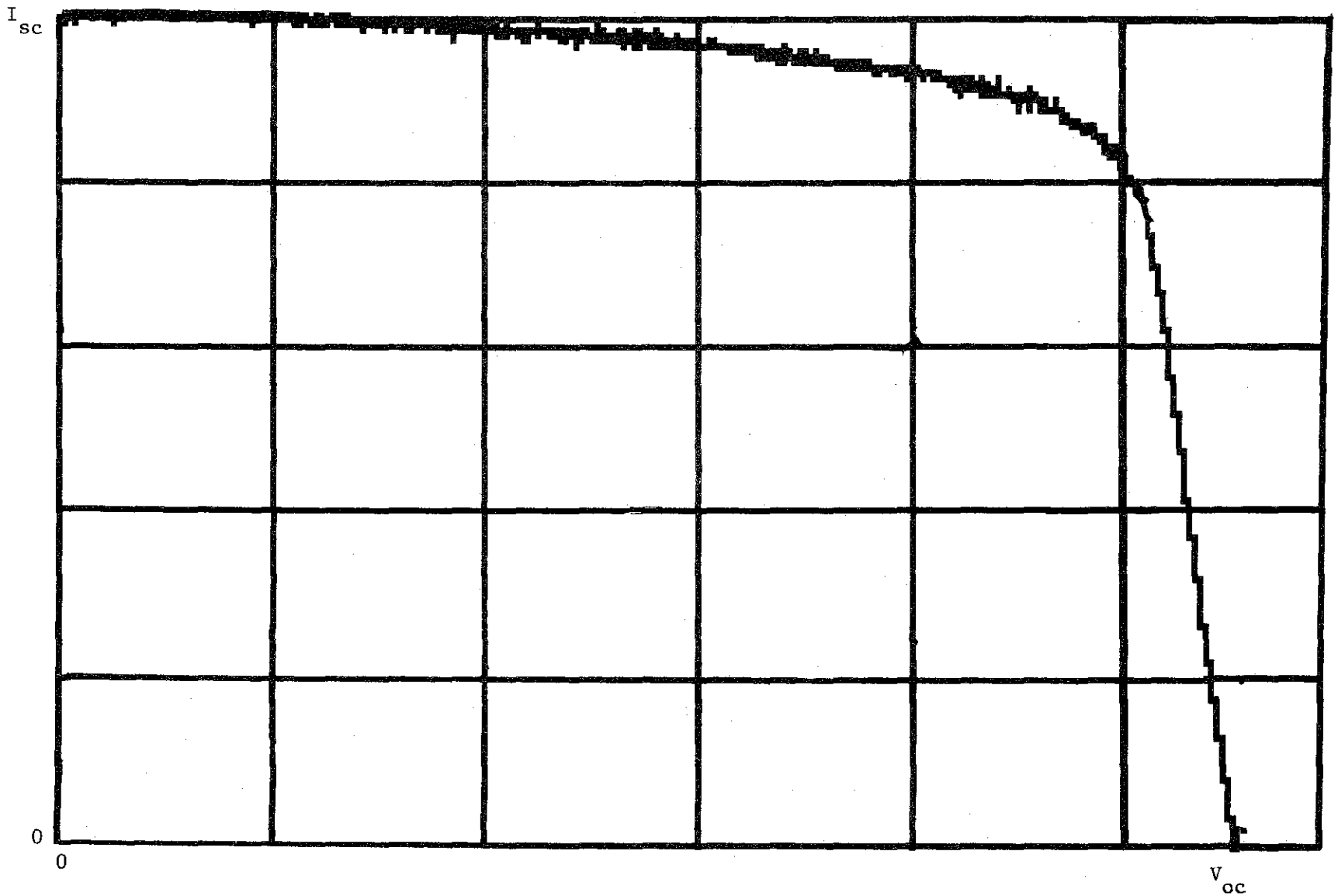

Fig. 2. I-V characteristic of the power supply.

Dimensions and weights

The opposite figure shows the overall dimensions of the pump. For more detailed information concerning the installation on dug wells and boreholes, refer to the installation manual.

The weights and dimensions of the pump and its main parts are as follows:

Complete pump (for 2.5 m depth)	:	120 kg
uPVC riser + rod (per length of 10 m)	:	23 kg
Steel box incl. stay bolts (optional)	:	65 kg

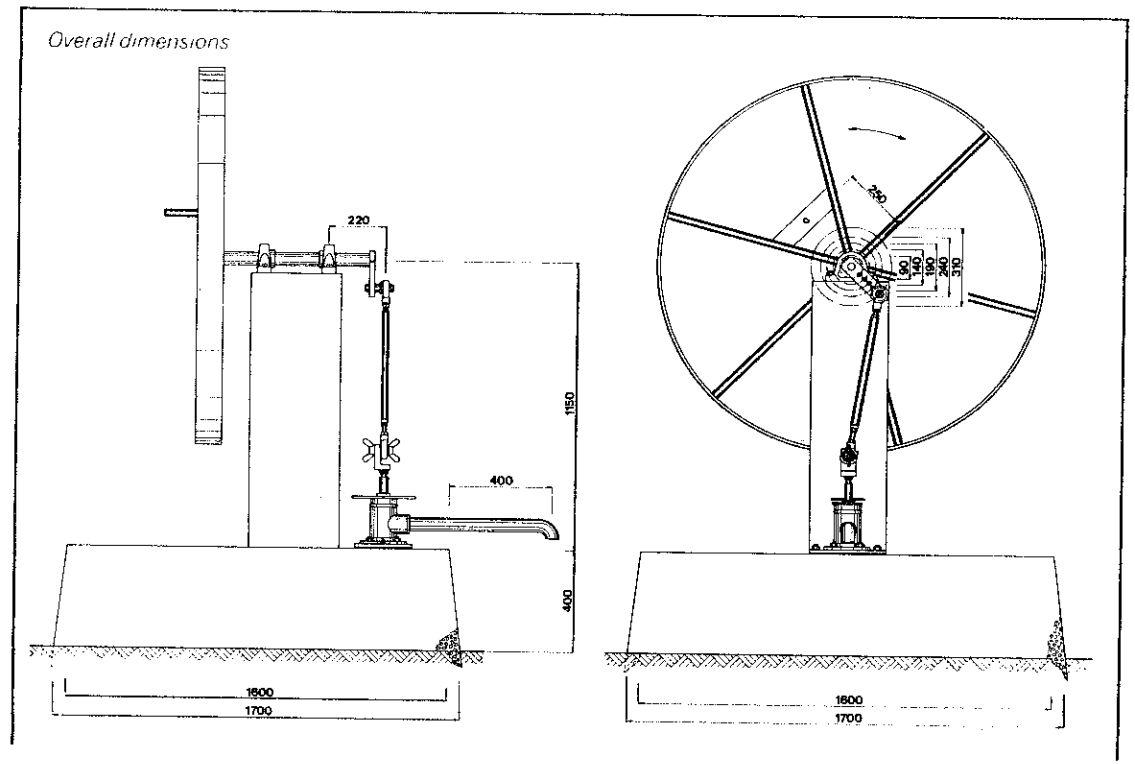

Figure 3. Sketch of the Volanta handpump (from brochure)

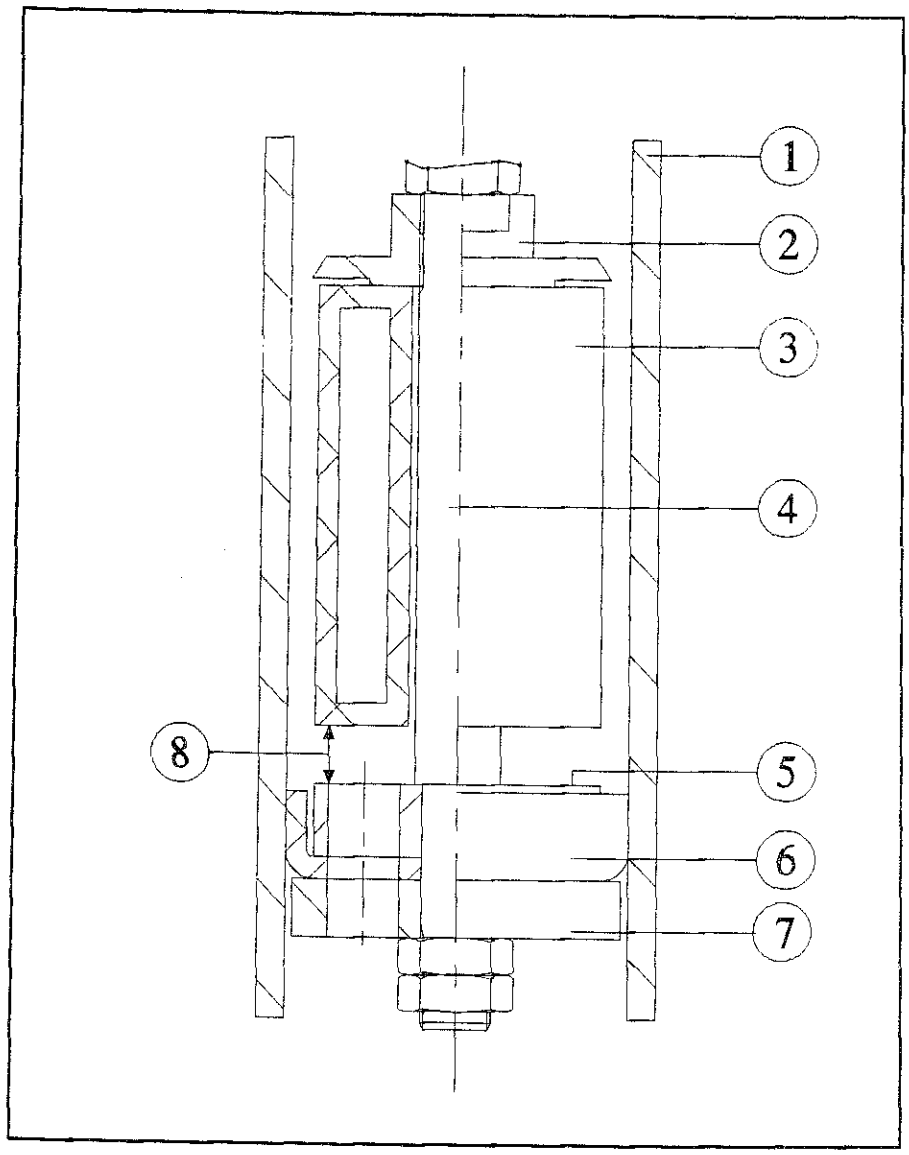

1. pump cylinder (ϕ_o= 50 mm)
2. upper valve stop (ρ = 45 mm)
3. TUE-matching valve; polypropylene (ρ = 951 kg/m^3) (ϕ_o = 42 mm, height 120 mm, mass 62.2 gram)
4. pumprod
5. upper part of the piston
6. leather cup
7. lower part of the piston

} all equipped with 6 holes (ϕ10mm) on a circle of 26 mm.

8. valve lifting height. This height is adjustable and determines the closure velocity.

Figure 4 Sketch of the piston and matching valve (from TUE).

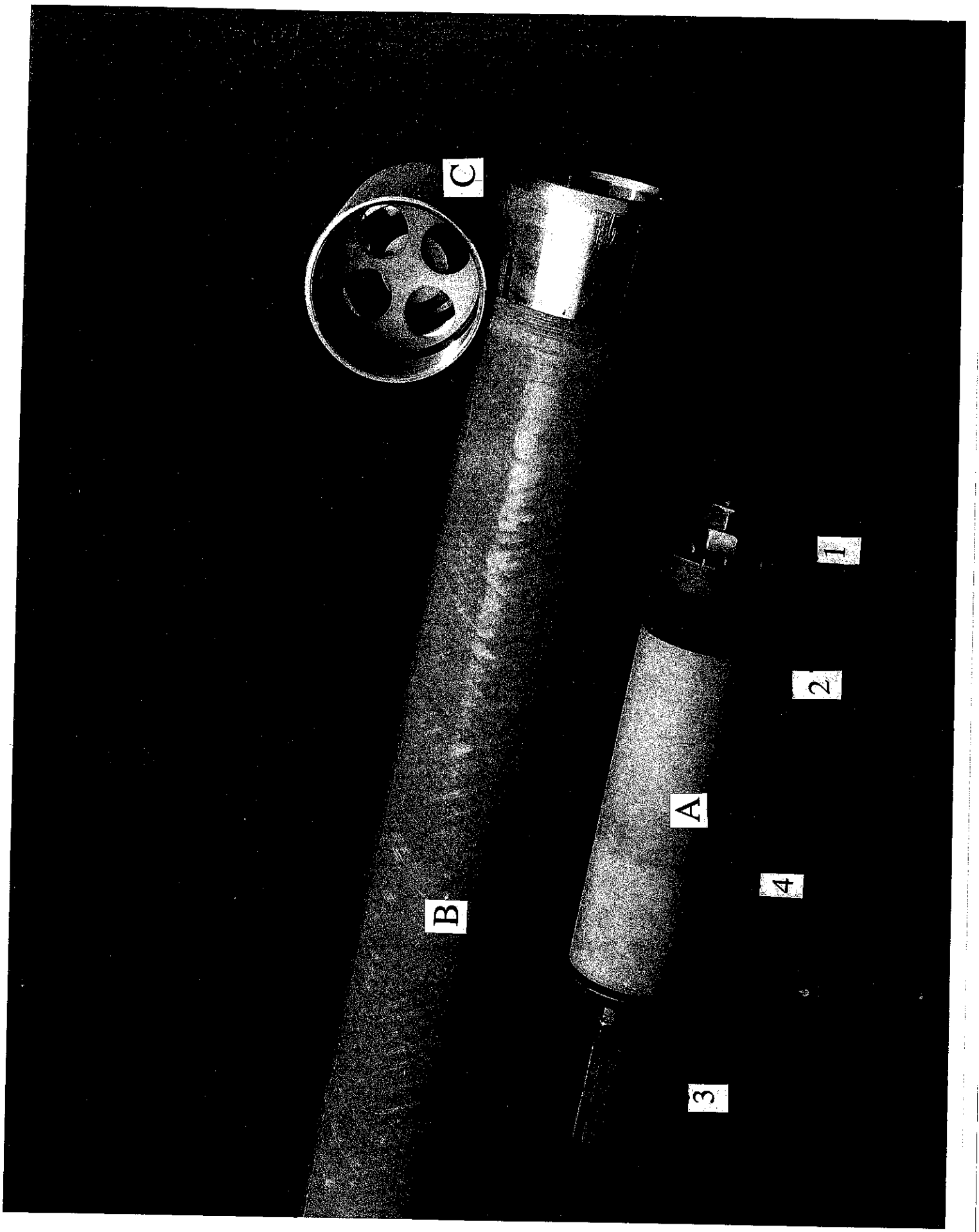

Photograph
Piston pump with matching valve
A: Piston with valve seat (1), leather (seal) cup (2), floating valve (4) and piston rod connection (3).
B: Pump cylinder
C: Foot valve

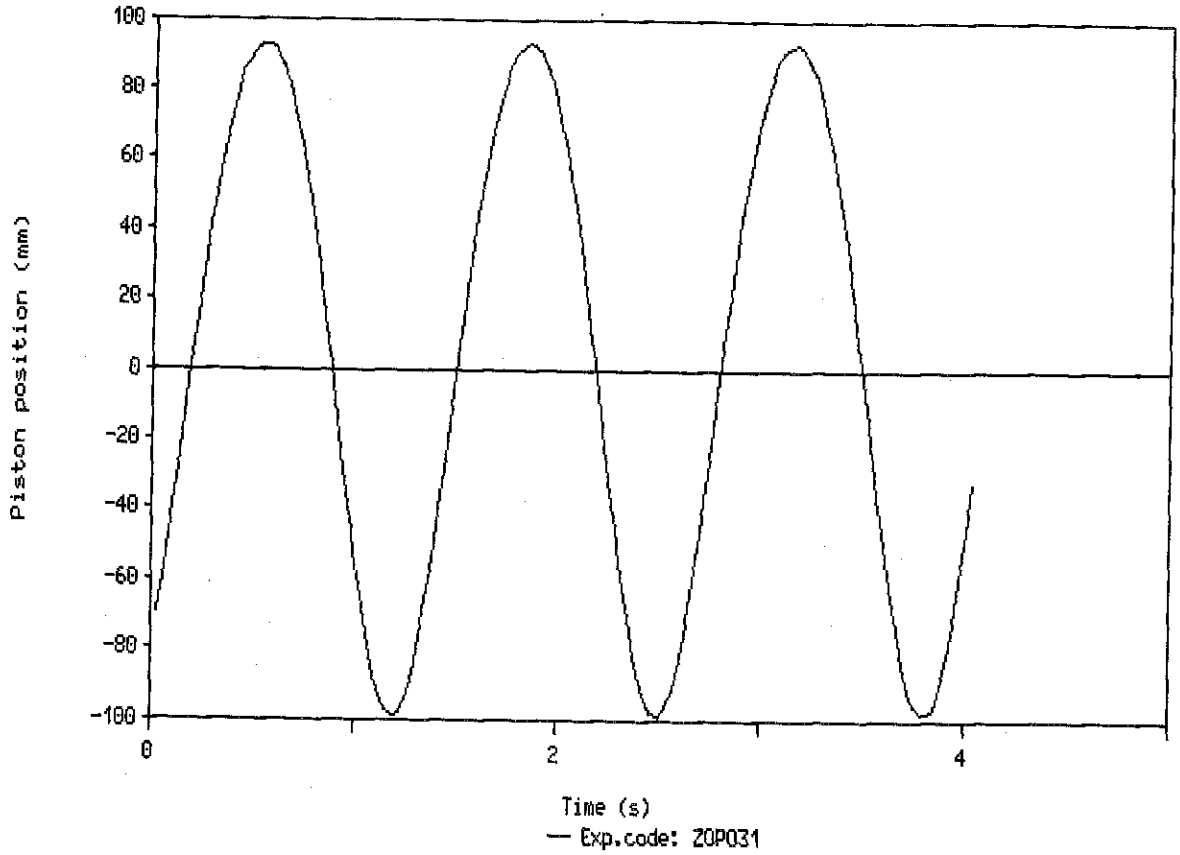

Fig. 5.1 Piston position during experiment ZOP031

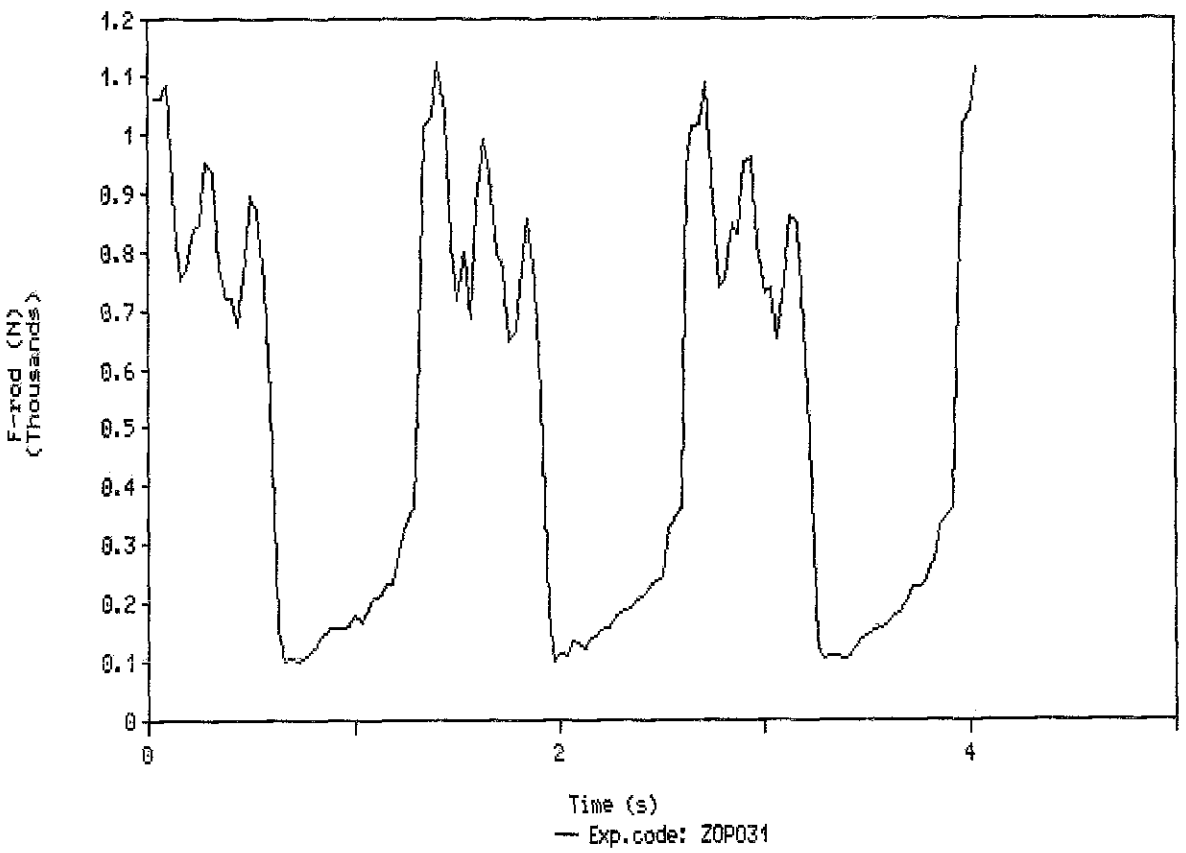

Fig. 5.2 Pumprod force during experiment ZOP031
(static force of the water on the piston: 492 N)

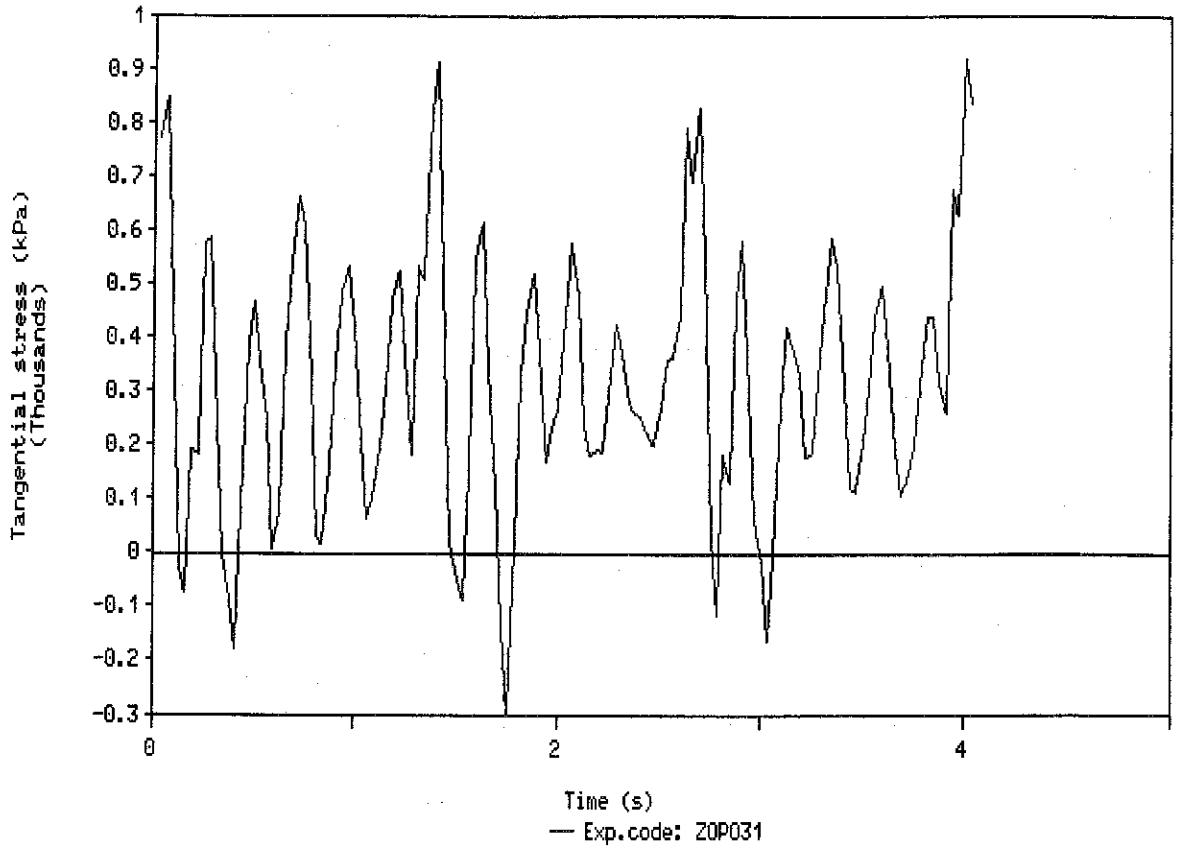

Fig. 5.3 Tangential stress in the rising main during experiment ZOP031

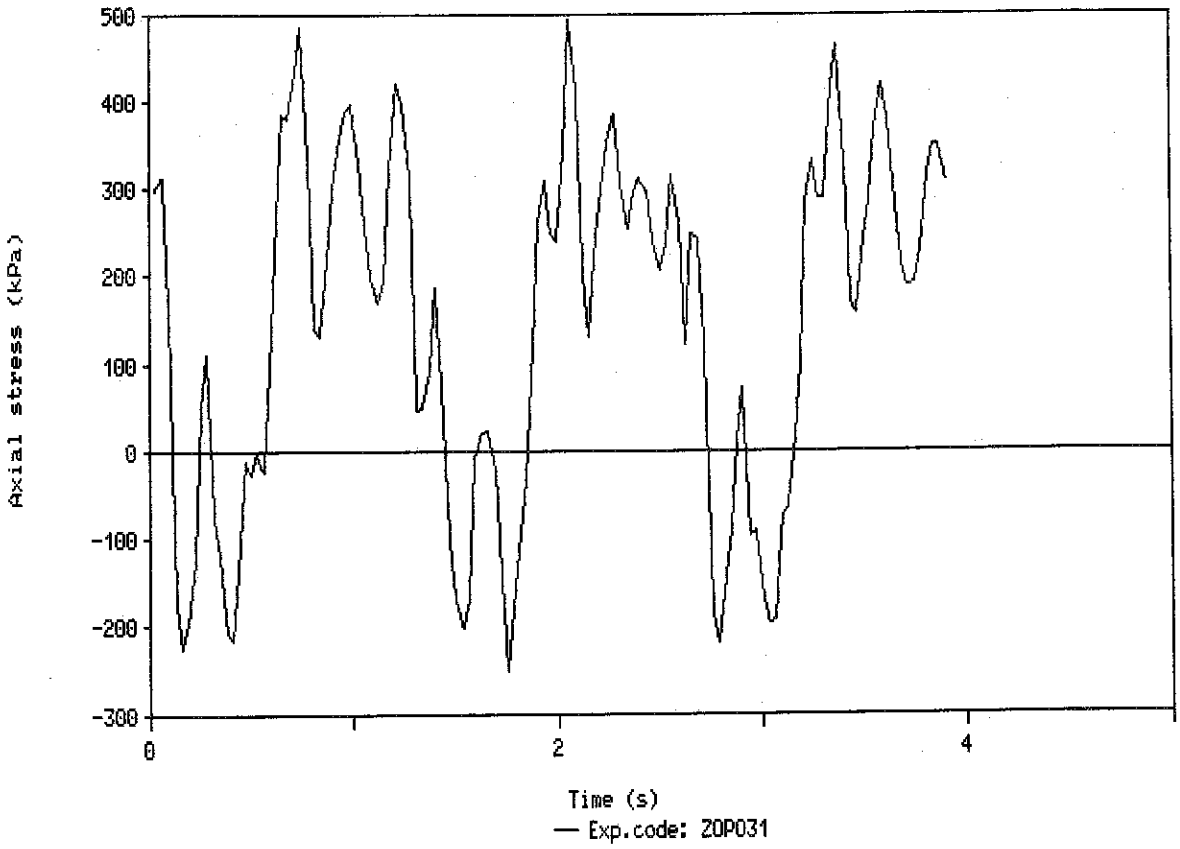

Fig. 5.4 Axial stress in the rising main during experiment ZOP031

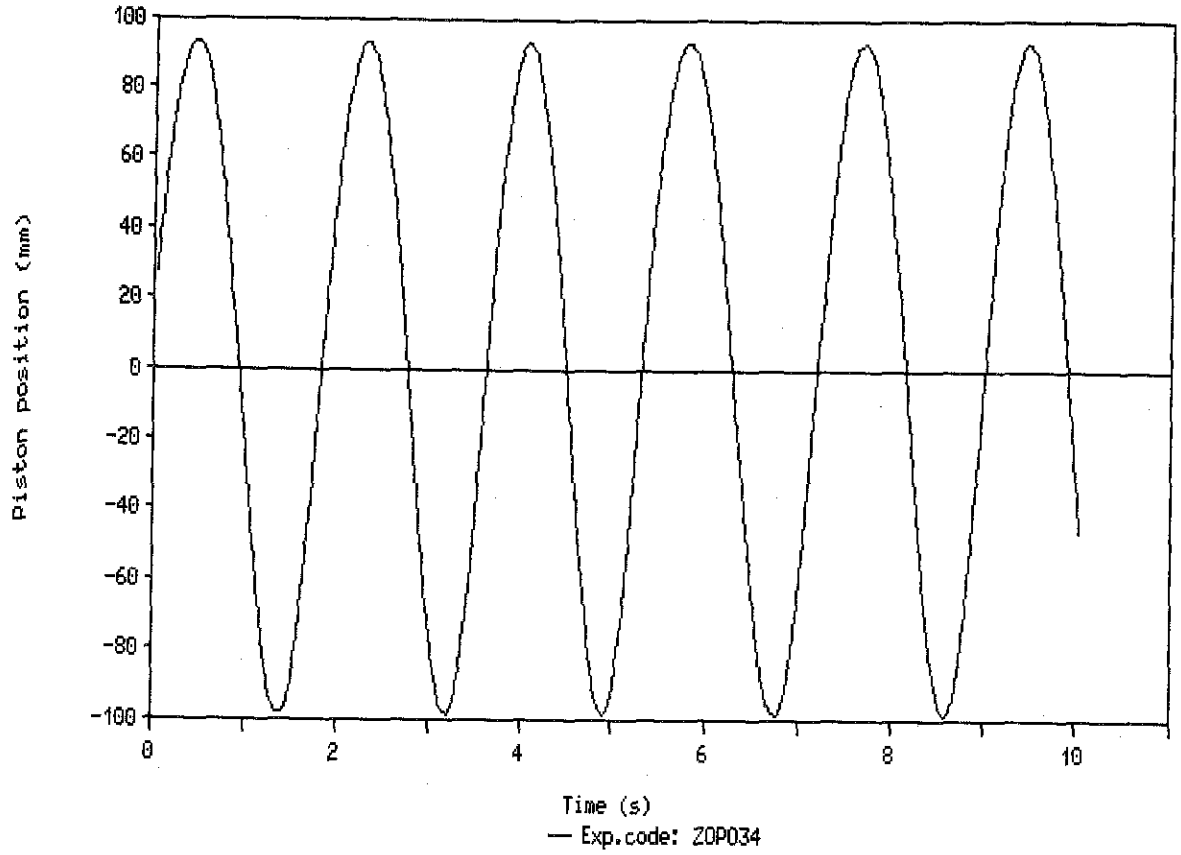

Fig. 5.5 Piston position during experiment ZOP034

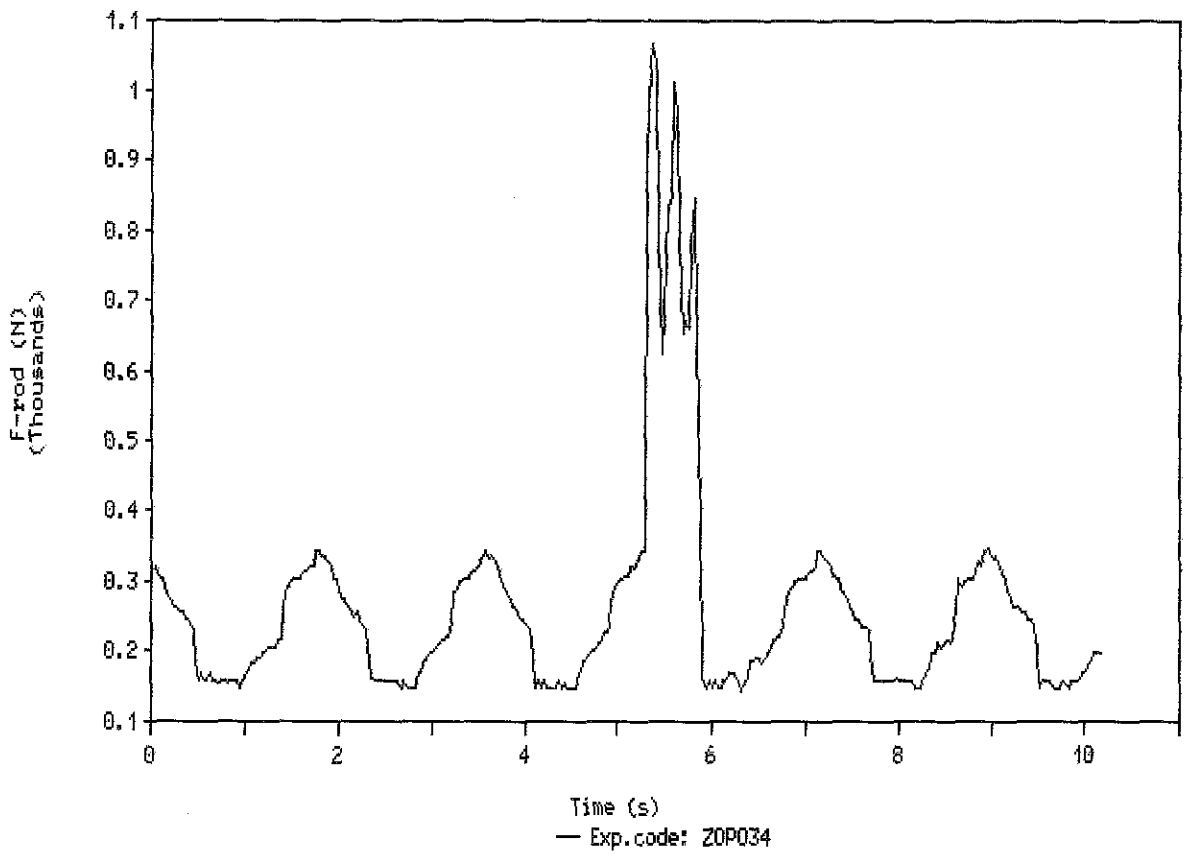

Fig. 5.6 Pumprod force during experiment ZOP034
(static force of the water on the piston: 492 N)

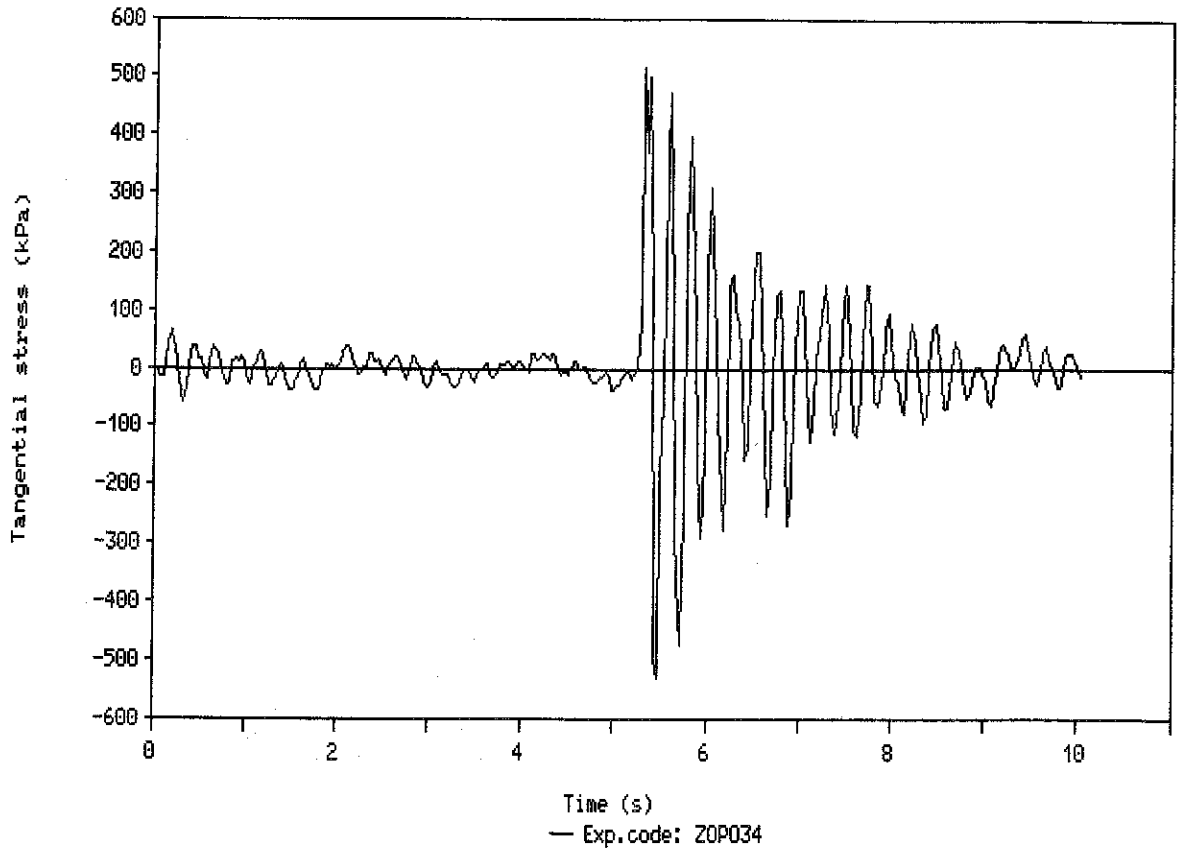

Fig. 5.7 Tangential stress in the rising main during experiment ZOP034

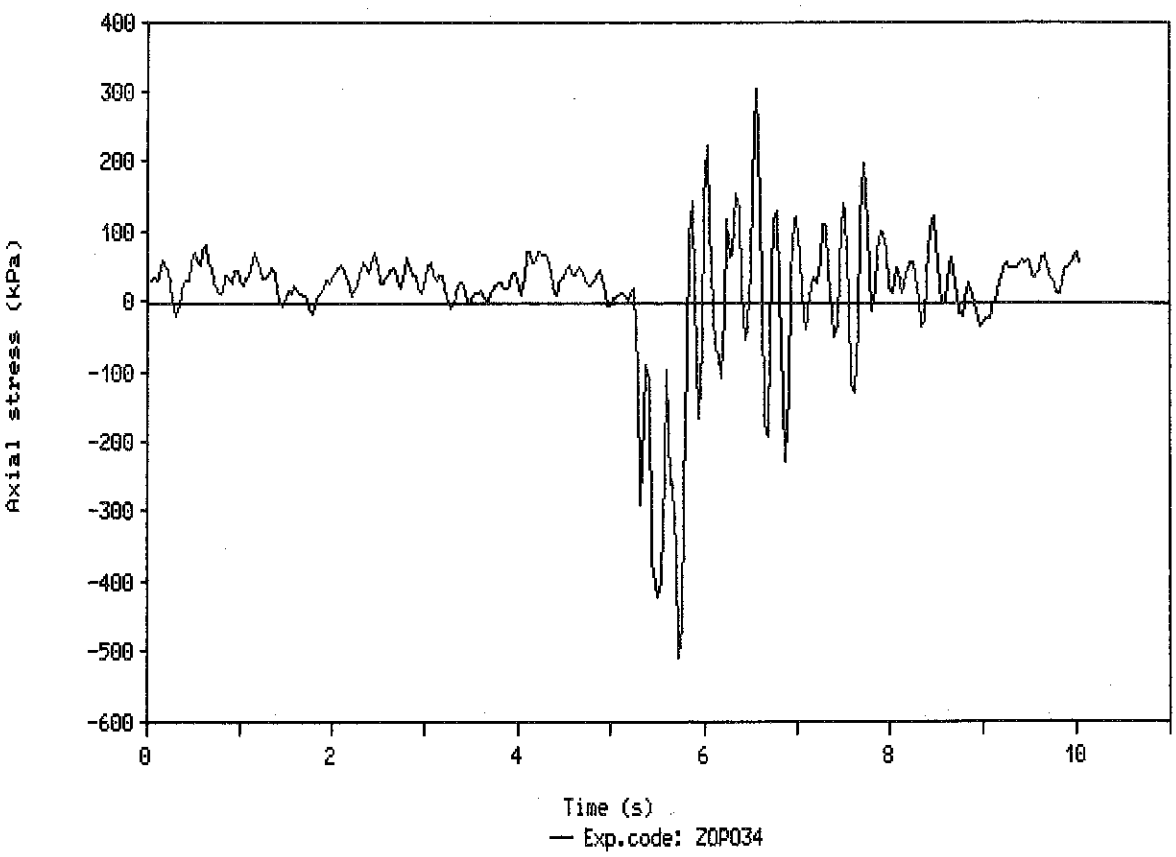

Fig. 5.8 Axial stress in the rising main during experiment ZOP034

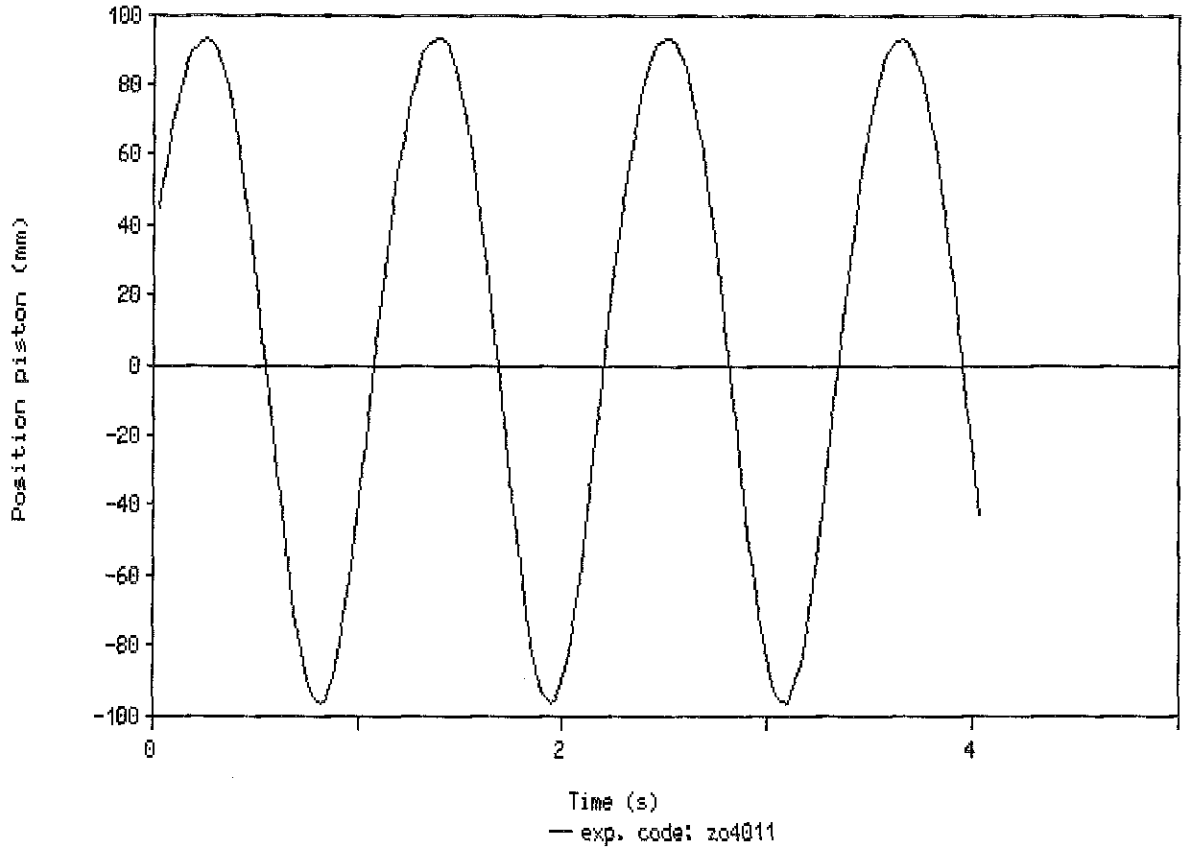

Fig. 6.1 Piston position during experiment ZO4011

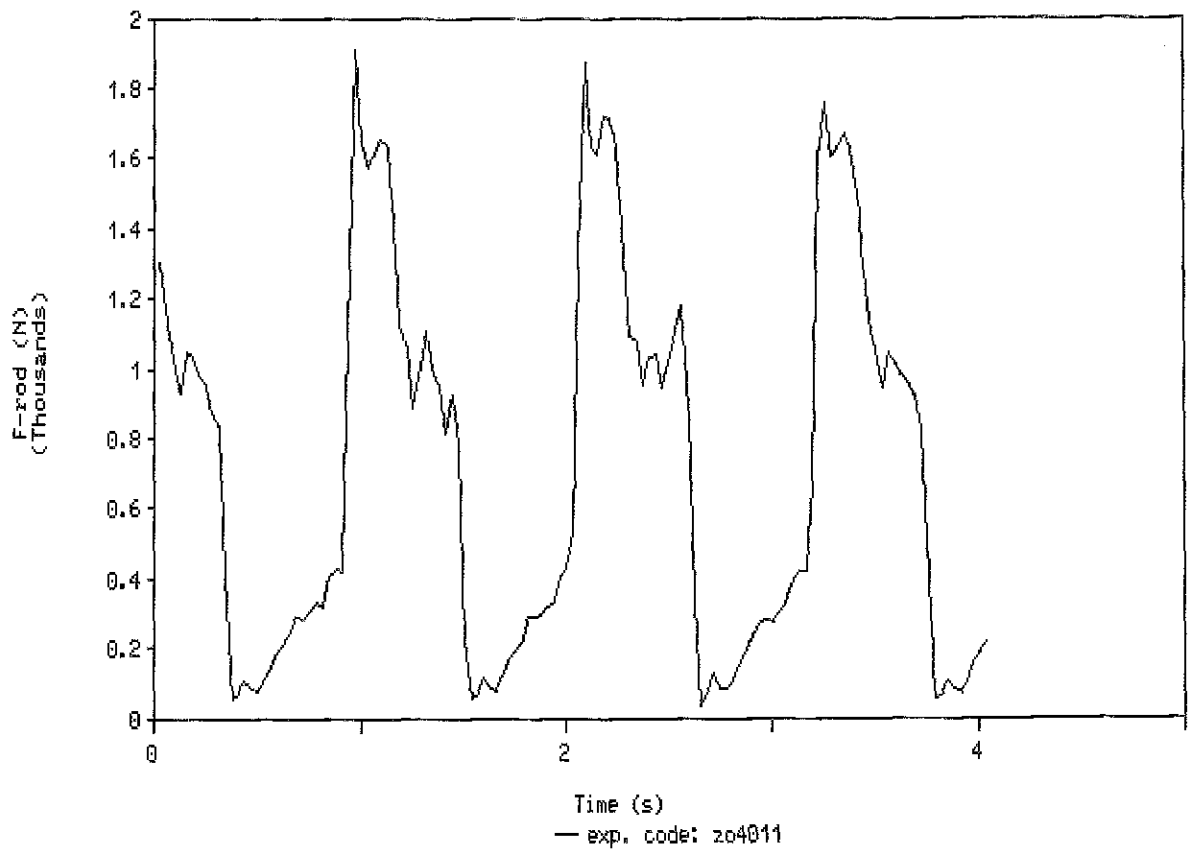

Fig. 6.2 Pumprod force during experiment ZO4011
(static force of the water on the piston: 860 N)

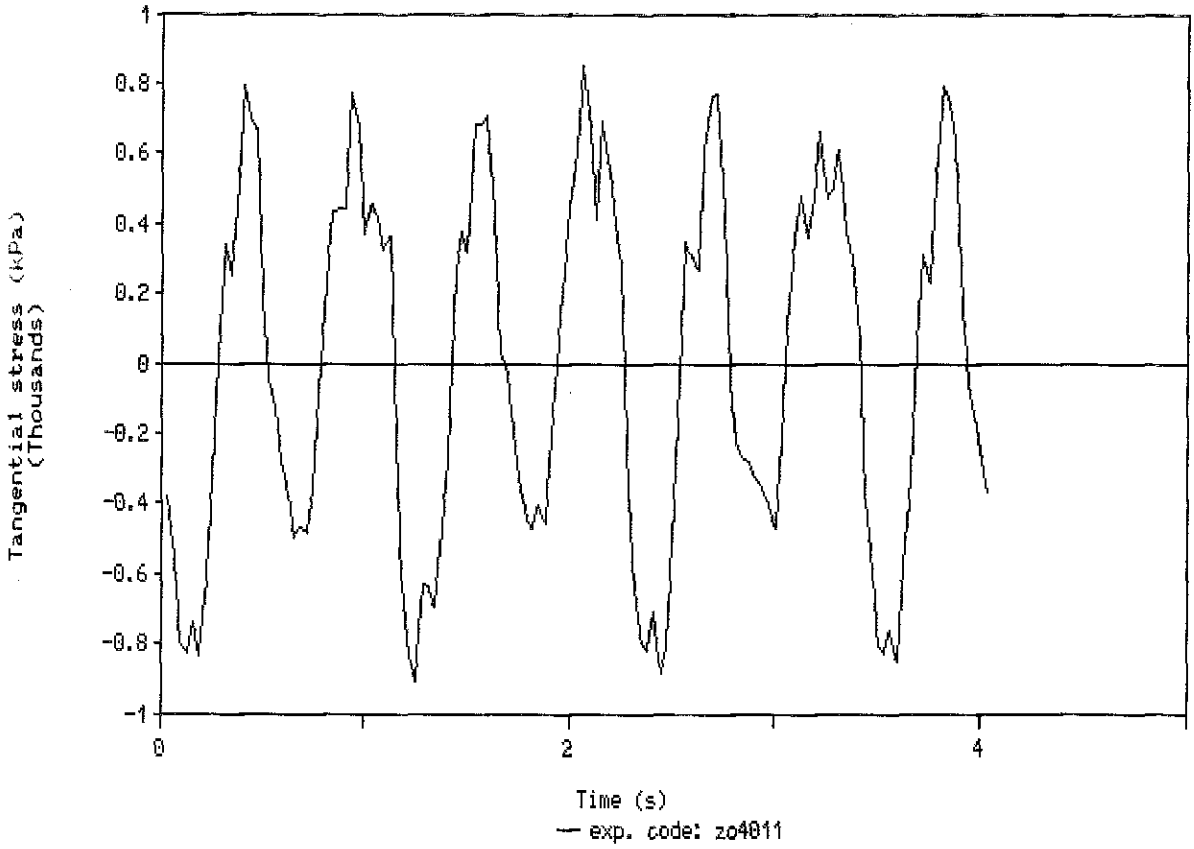

Fig. 6.3 Tangential stress in the rising main during experiment ZO4011

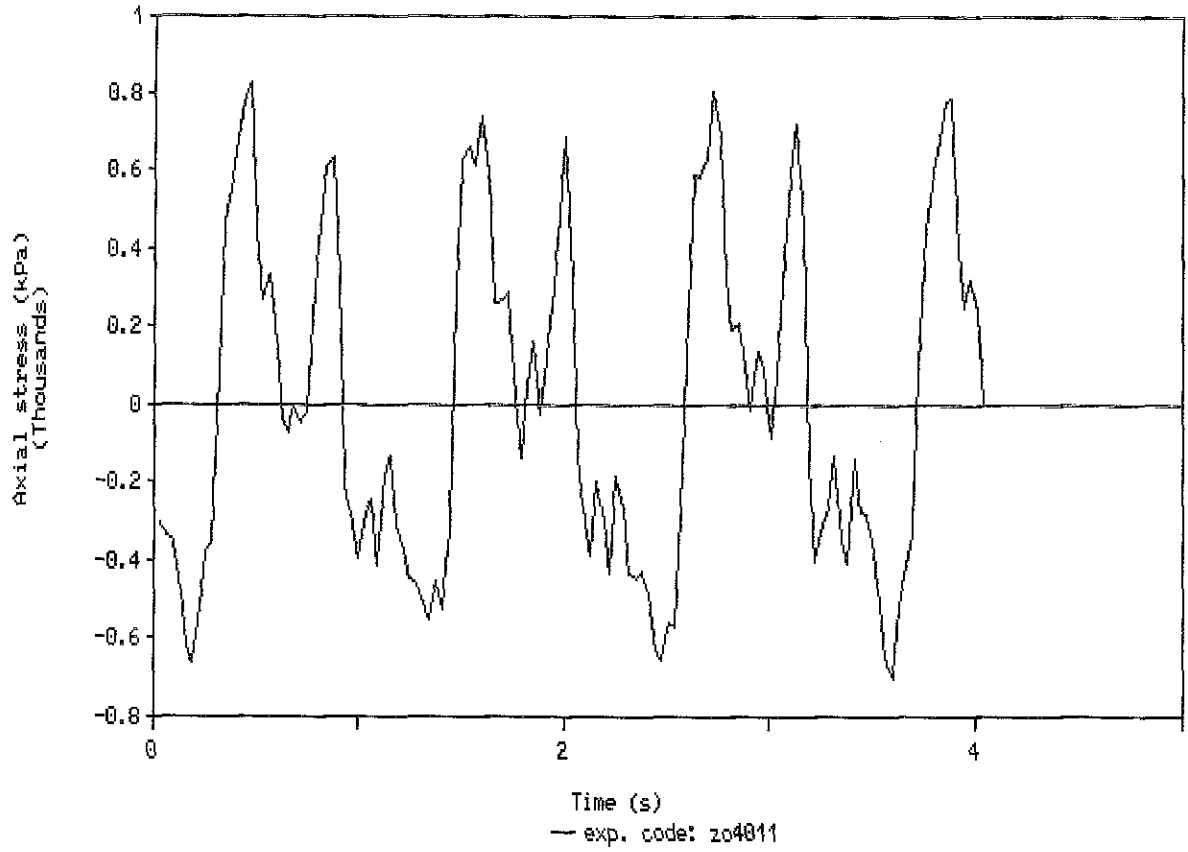

Fig. 6.4 Axial stress in the rising main during experiment ZO4011

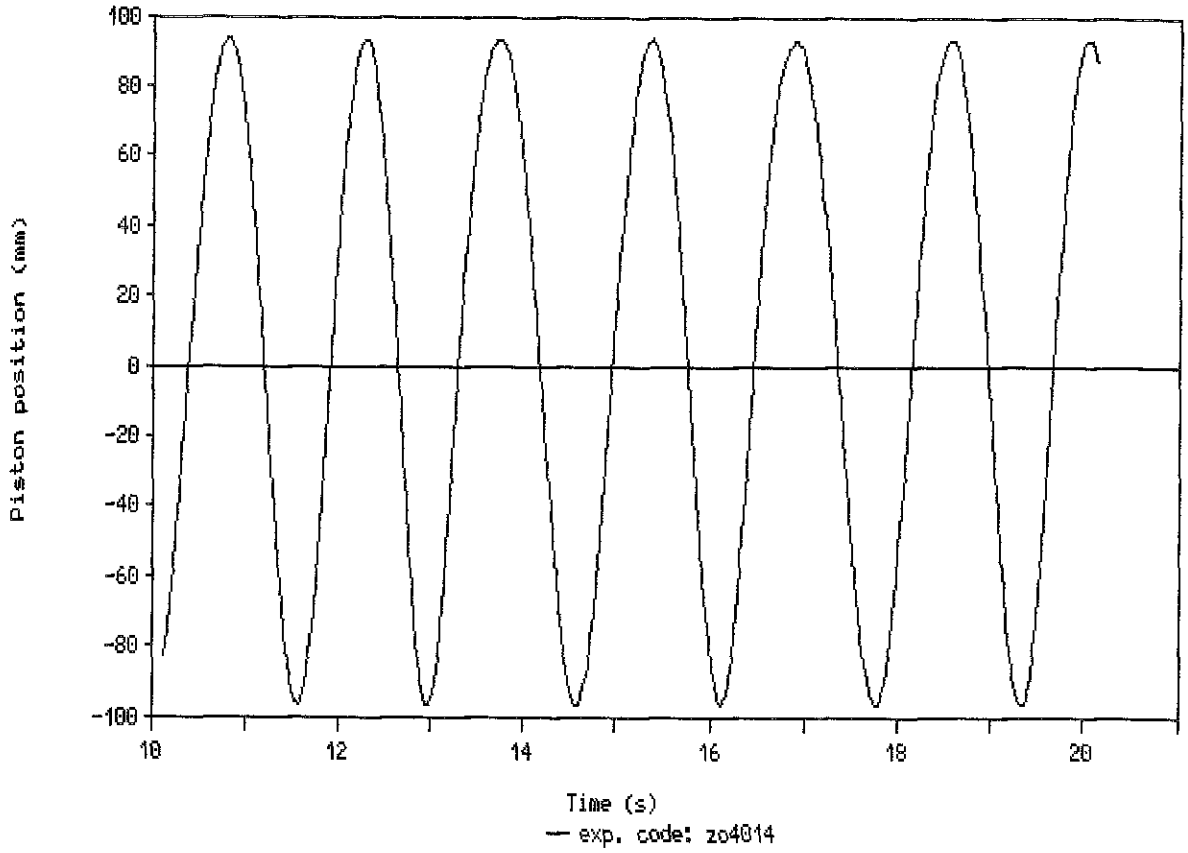

Fig. 6.5 Piston position during experiment ZO4014

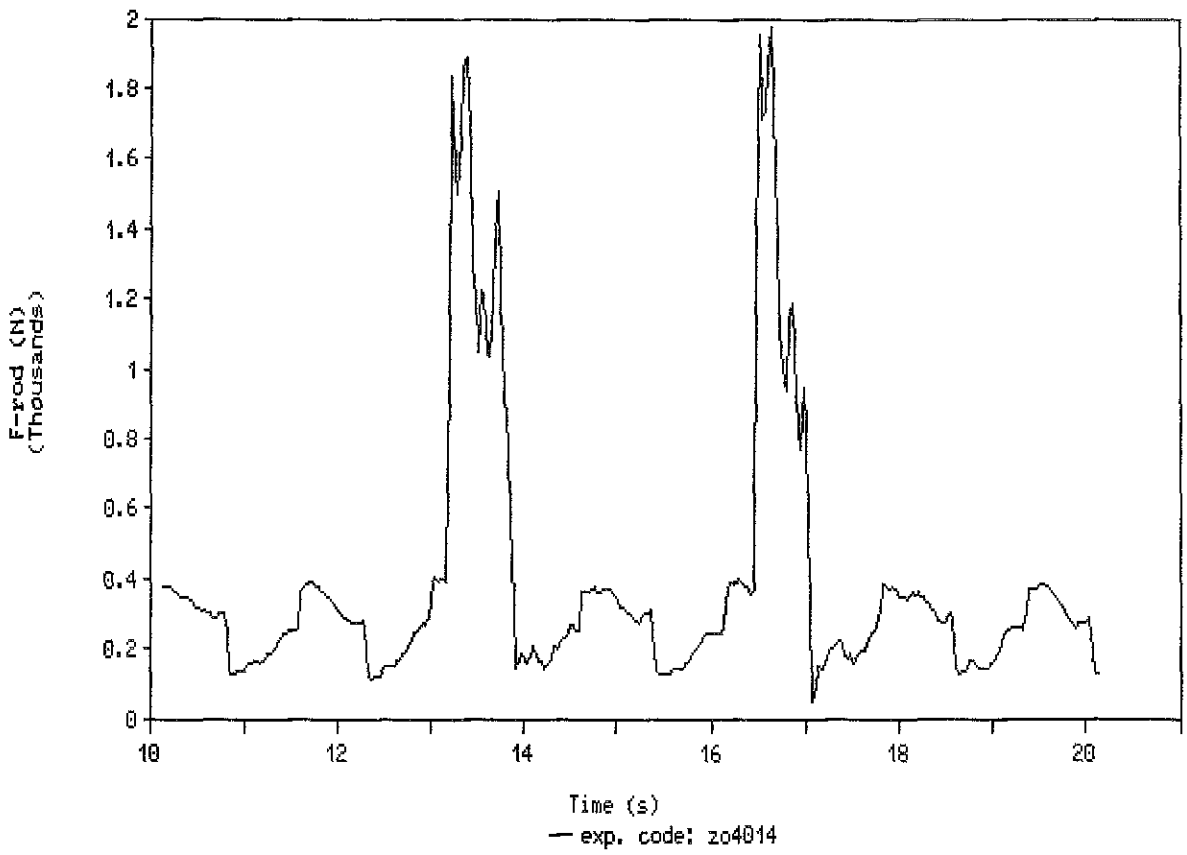

Fig. 6.6 Pumprod force during experiment ZO4014
(static force of the water on the piston: 860 N)

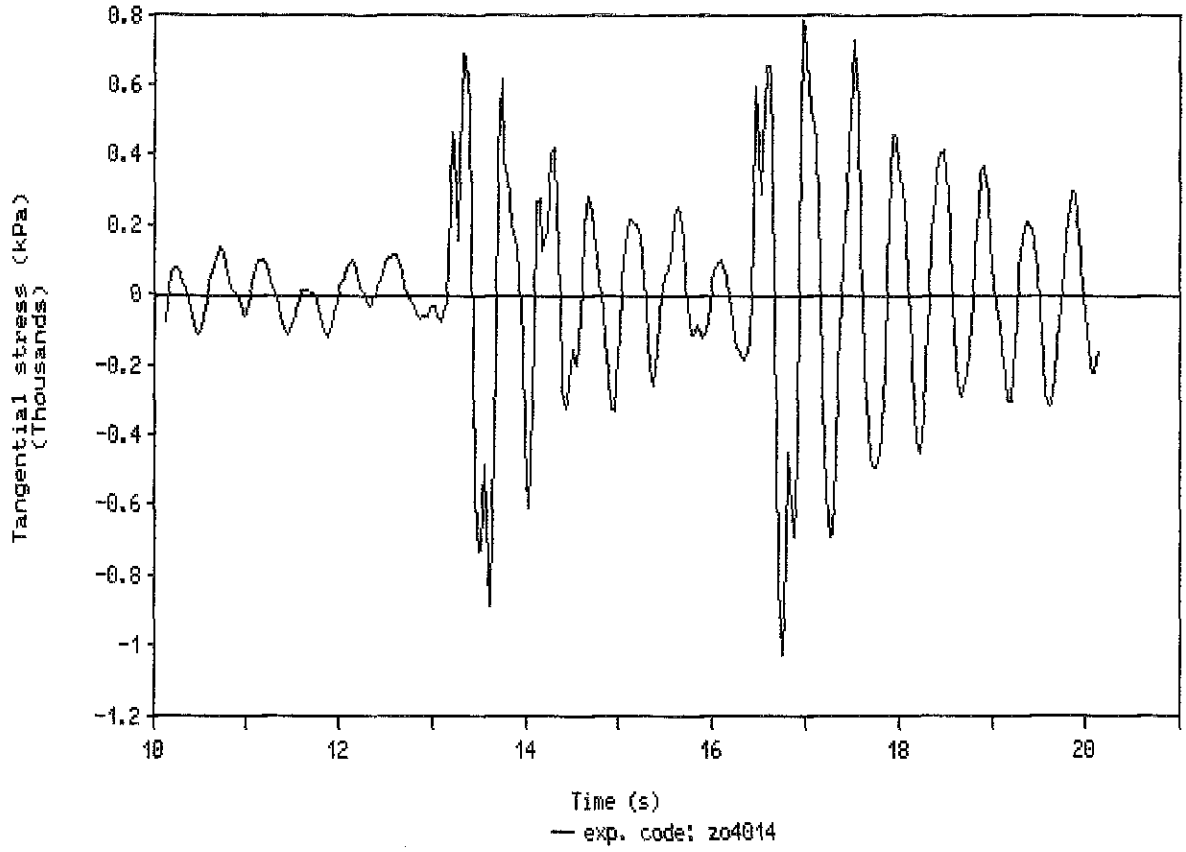

Fig. 6.7 Tangential stress in the rising main during experiment ZO4014

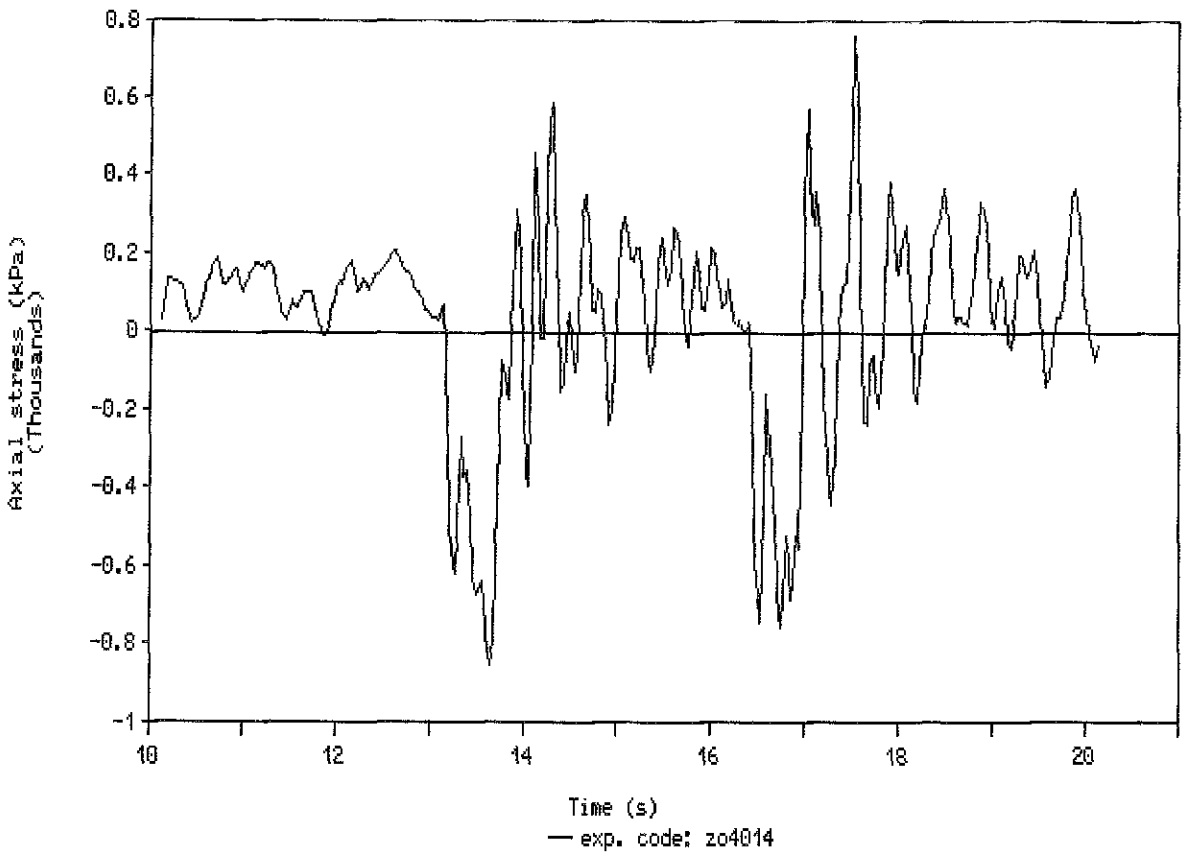

Fig. 6.8 Axial stress in the rising main during experiment ZO4014

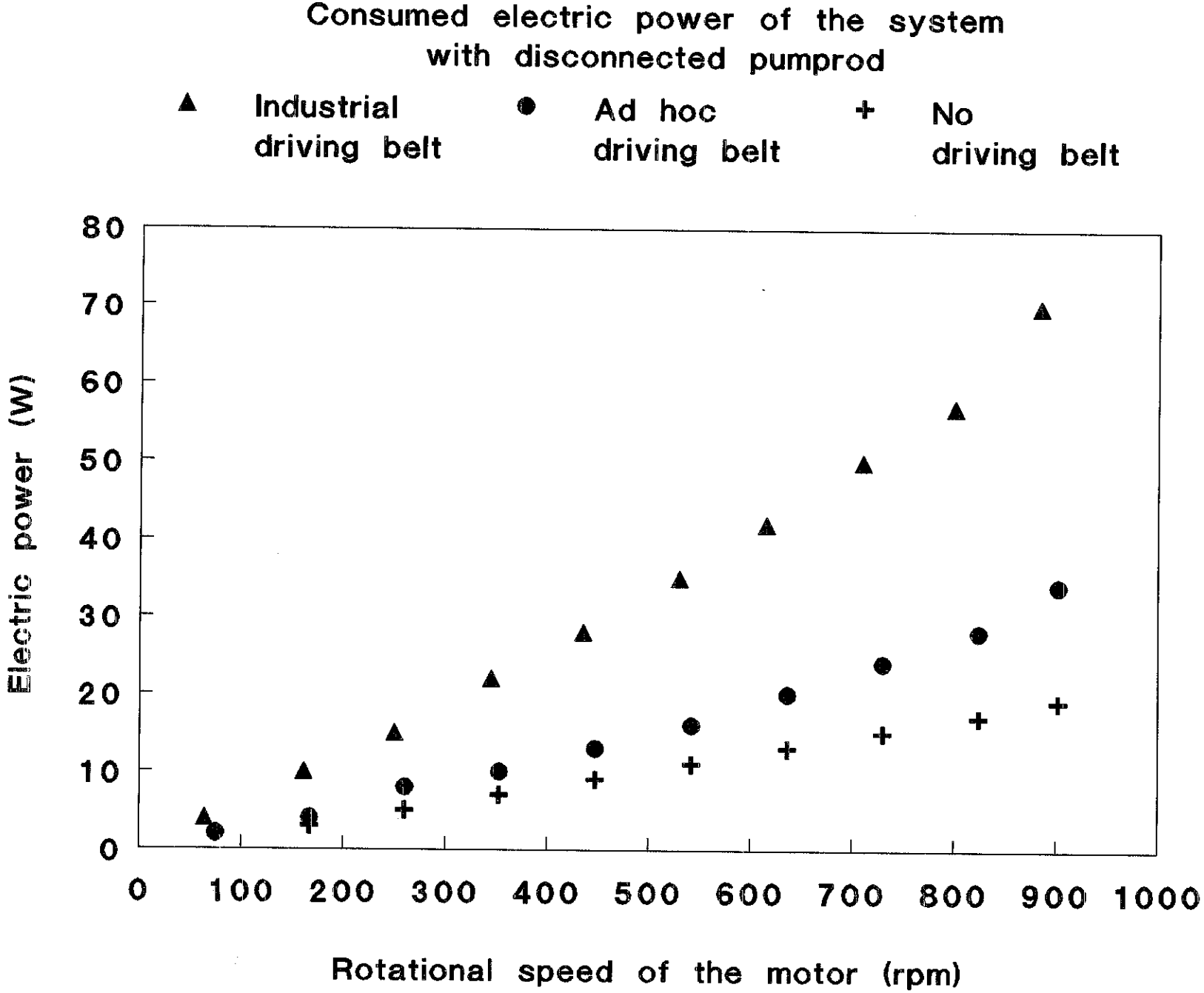
Consumed electric power of the system
with disconnected pumprod
▲ Industrial driving belt
● Ad hoc driving belt
+ No driving belt
Electric power (W)
0
10
20
30
40
50
60
70
80
0 100 200 300 400 500 600 700 800 900 1000
Rotational speed of the motor (rpm)

Fig. 7

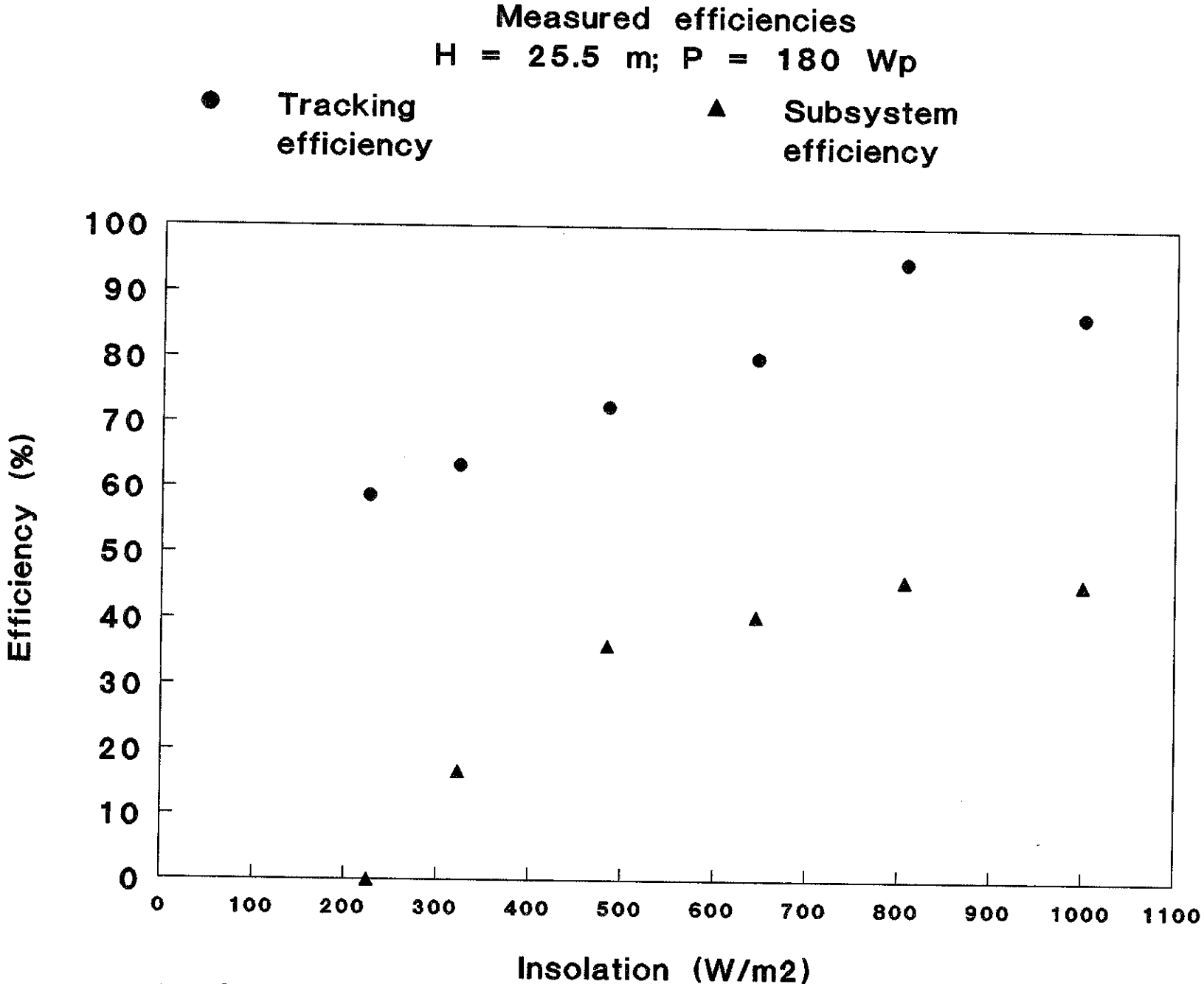
Measured efficiencies
H = 25.5 m; P = 180 Wp
Tracking efficiency
Subsystem efficiency
Efficiency (%)
100
90
80
70
60
50
40
30
20
10
0
0
100
200
300
400
500
600
700
800
900
1000
1100
Insolation (W/m2)

Fig. 8

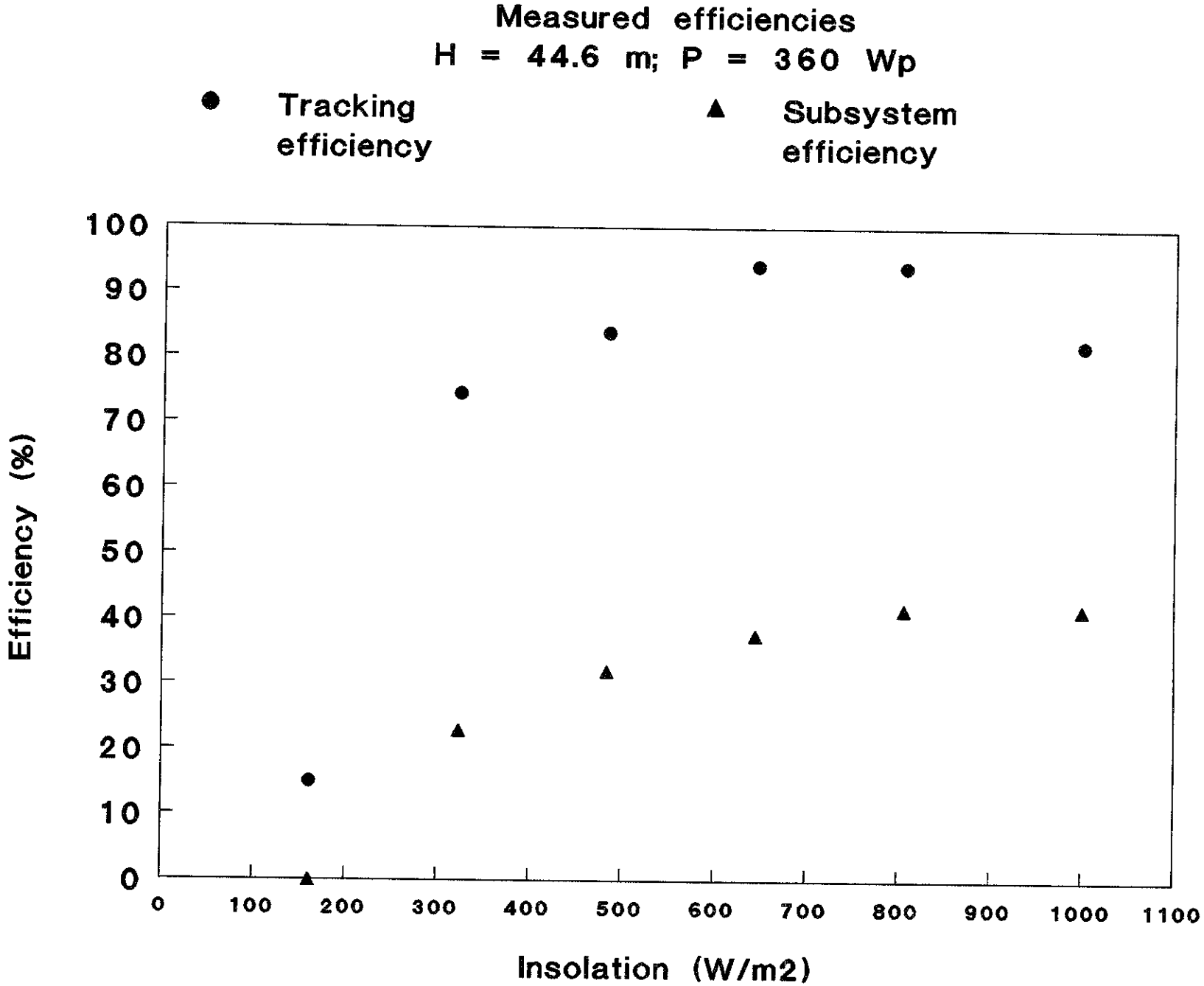
Measured efficiencies
H = 44.6 m; P = 360 Wp
Tracking efficiency
Subsystem efficiency
Efficiency (%)
100
90
80
70
60
50
40
30
20
10
0
0
100
200
300
400
500
600
700
800
900
1000
1100
Insolation (W/m2)

Fig. 9

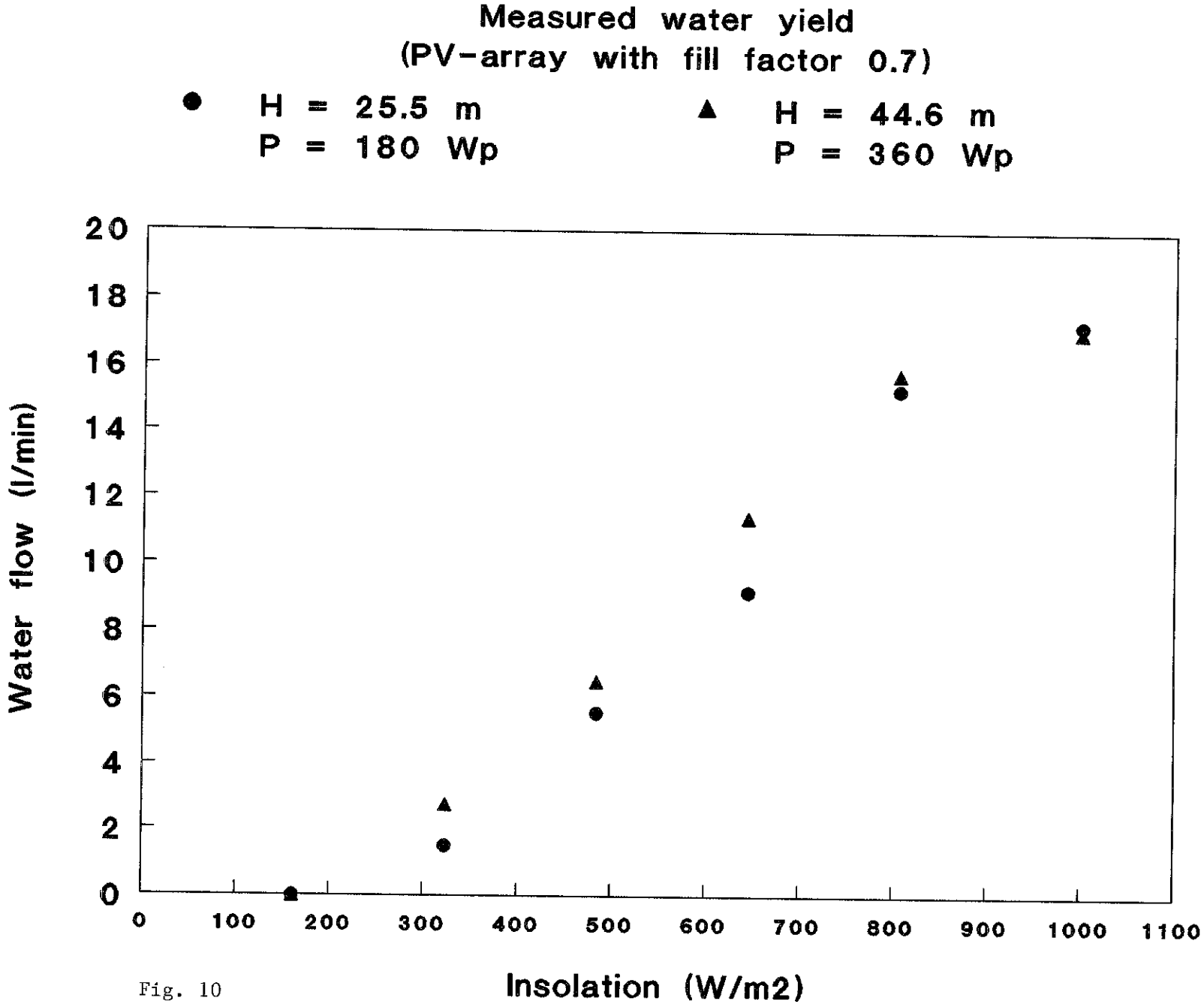
Measured water yield
(PV-array with fill factor 0.7)
H = 25.5 m
P = 180 Wp
H = 44.6 m
P = 360 Wp
Water flow (l/min)
0
2
4
6
8
10
12
14
16
18
20
0
100
200
300
400
500
600
700
800
900
1000
1100
Insolation (W/m2)

Fig. 10

APPENDIX A SUMMARIZED DESIGN RULES FOR HANDPUMPS UNDER FATIGUE CONDITIONS (from REF1)

IV.1 STAINLESS STEEL

IV.1.1. Stainless steel AISI 304

For pump rods that are normally submerged in fresh water the fatigue strength goes down with an increasing number of cycles. The ultimate fatigue strength of both annealed and 98% cold worked stainless steel AISI 304 is given in Figure 5.1.

The ultimate fatigue strength[5] of smooth stainless steel AISI 304 in fresh water[6] is

	200,000 cycles	100 million cycles
annealed AISI 304	240 N/mm^2	170 N/mm^2
98% cold worked AISI 304	860 N/mm^2	790 N/mm^2

For a type of stainless steel that has only been partly cold worked, the fatigue strength can be found by linear interpolation between the values of 0% and 98%.

IV.1.2. Notched stainless steel AISI 304

The notches for which the pump rods generally have to be designed are notches formed by grooves of a thread.
As a rule of thumb the following values can be used:

- for mechanically cut thread $K_t \approx 3$ (IV.1)
- for rolled thread $K_t \approx 2$ (IV.2)

For *annealed stainless steel AISI 304* $q = 0.3$ for $K_t < 4$ (IV.3)

For *cold worked (98%) stainless steel AISI 304*
$q = 0.7$ for $K_t < 4$ (IV.4)

In all cases: $K_f = 1 + q(K_t - 1)$ (see paragraph 5.5.5) (IV.5)

Safety factor

In view of the range of values for K_f found in literature, as well as the incompleteness of data about notches, it is preferable to take a safety factor of 2 for thread under load:

safety factor = 2

---

5 This is valid for alternating axial stresses (combined tension and bending) in the pump rod, which is normally the case. It is not valid for torsion.

6 In aggressive water lower values apply.

IV.1.3. Summarized design procedure

To obtain the design strength of stainless steel AISI 304 with thread, the following procedure can be followed:

Data to be given:
- the material, stainless steel AISI 304
- the treatment: annealed or cold worked, in %
- the plain fatigue stress
- the type of thread, with K_t value

In most cases, the value for K_t of thread is given in handbooks; if not, determine:
- K_t using equations (IV.1) or (IV.2)
- K_f using equations (IV.3), (IV.4) or (IV.5)

Choose a desirable lifetime for the pump rod, say 10 years. With Figure 5.6 this gives a number of cycles of about 10^8 (100 million cycles) supposing the pump is used as indicated. With the same figure the plain fatigue strength can be found, using the lines for fresh water (which take the corrosion effect into account only partly). The ultimate fatigue strength and design fatigue strength can then be calculated, as follows:

- ultimate fatigue strength $= \dfrac{\text{plain fatigue strength}}{K_f}$

- design fatigue strength $= \dfrac{\text{ultimate fatigue strength}}{\text{safety factor}}$

IV.1.4 Example calculation

Assume mechanically cut thread BSF (r = 0.135) on annealed stainless steel AISI 304 pump rods.
From data books the value $K_t = 3.3$ can be derived, resulting in a factor $K_f = 1.7$, according to equation (IV.5)[7].

At a lifetime of 10 years (10^8 cycles) the plain fatigue stress then is found to be 170 N/mm^2.
This gives an ultimate fatigue strength of 170/1.7 = 100 N/mm^2.
Taking into account a safety factor of 2, as recommended by Beekman and de Jongh, the design fatigue strength becomes: 100/2 = 50 N/mm^2.

[7] When no data books are available, the value proposed under (IV.1) and equation (IV.5) would give $K_t = 3$ and $K_f = 1.6$, or: a negligible difference.

IV.2 PVC

Strength criteria

The brittle strength criteria for uPVC and rigid PVC for rising mains in handpumps, protected against direct sunlight[8] are:
fatigue strength (for 10^8 cycles):

- for smooth pipe 16.5 N/mm^2 (IV.6)
- for glued/threaded pipe 6.0 N/mm^2

For the S-N curve of smooth PVC see Figure 5.2.

Note:
For a threaded riser connection it is possible to estimate a fatigue strength, based upon the geometrical data of the thread cut on the pipe ends. First the stress concentration is calculated, and then, by using the notch sensitivity, the fatigue strength reduction factor. In the case of the SWN pump this results in a fatigue strength of about 6 N/mm^2.
However, it is very probable that during cutting of the thread small cracks have developed, with a root radius of about 10 μm. As a consequence, the fatigue strength will have been reduced to 2.5 N/mm^2!

Also in a cemented rising main similar cracks may occur, due to the action of the solvent in the glue. Since we have no information on the strength reduction factor in relation to the chemical activity of the glue in a period of 10 years (or 10^8 cycles), we propose to use the value of 2.5 N/mm^2 also for the fatigue strength of a cemented rising main. (Field experience indicates that this value is not too low.)

The maximum allowable load fluctuation amplitude on the riser can be found by multiplying the fatigue strength by the cross-sectional area of the riser.

---

[8] If PVC pipe is subjected to direct sunlight, the ultraviolet rays in the sunlight cause a vastly accelerated loss of strength of the pipe, which becomes brittle and discoloured (brown/blackish).

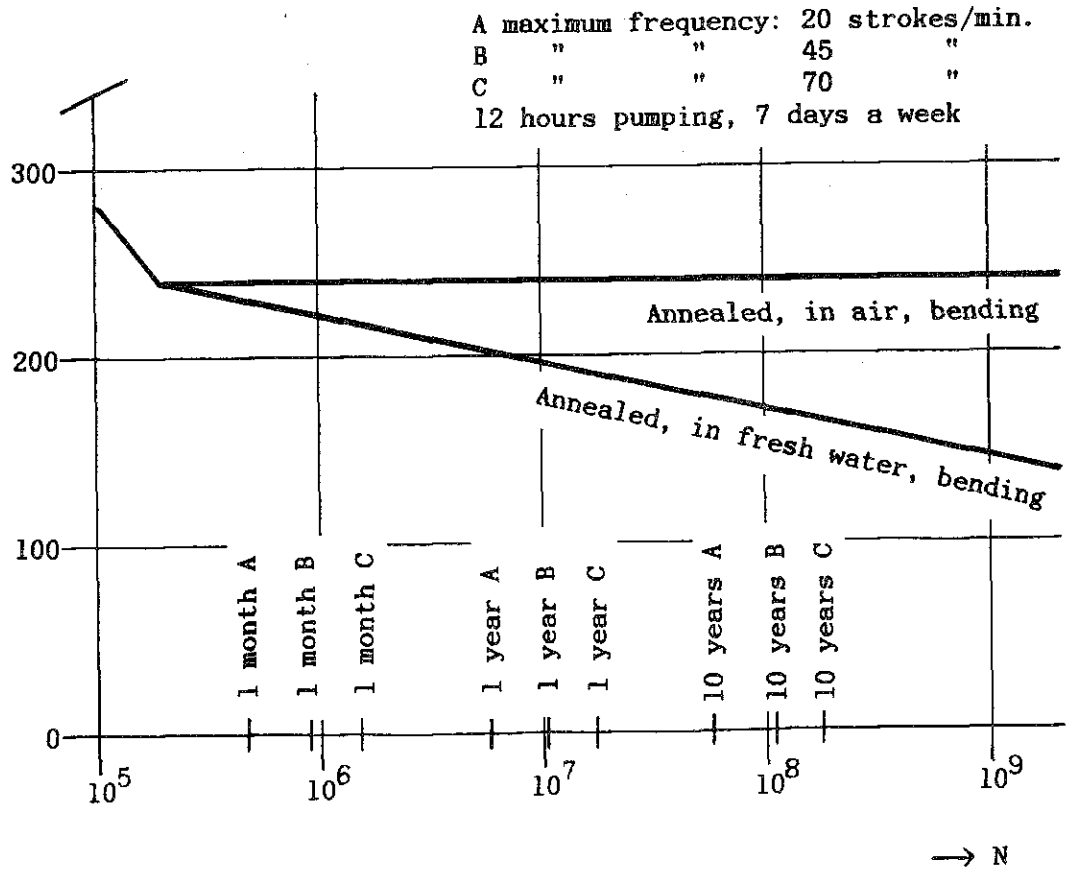

Figure 5.1 S-N curves for stainless steel AISI 304

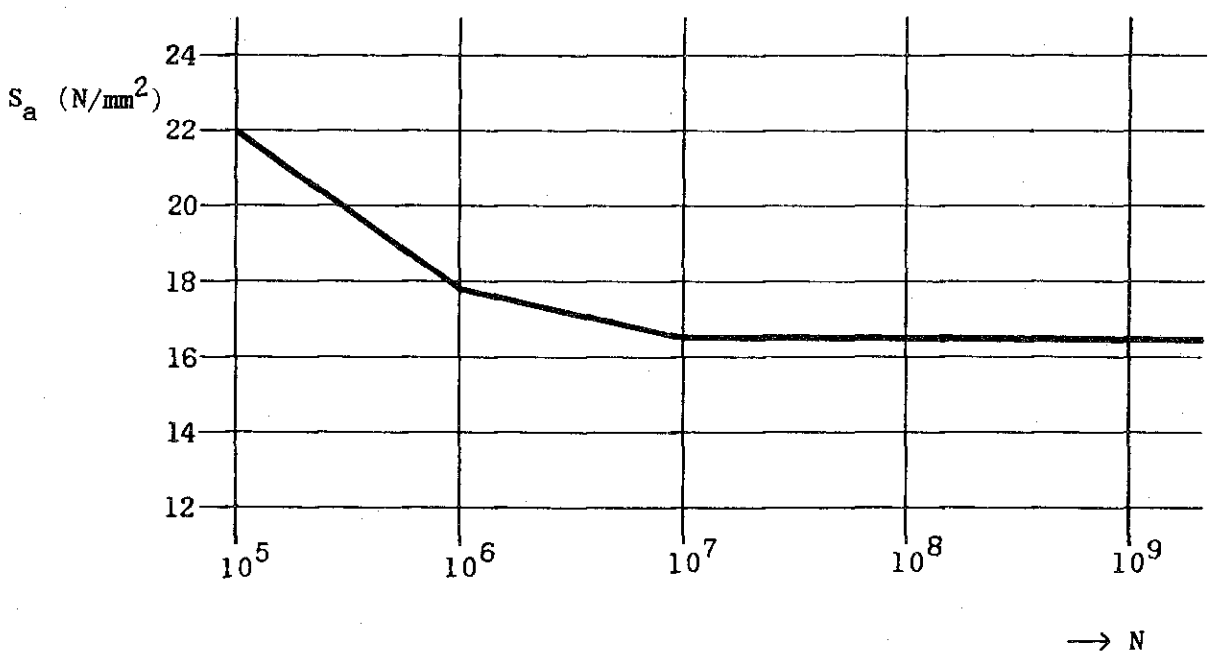

Figure 5.2 S-N curve of smooth PVC (uPVC and rigid PVC)

APPENDIX B
Calculation of the Stress Reserve Factor of the pumprod (L. Rademakers, ECN)

The material properties of AISI 304 are derived from Fig. 5.1 of appendix A, assuming "annealed" and used in "fresh water":

$$\log N = \log C - k \cdot \Delta S$$

with $k = 3.636 \cdot 10^{-8}$ and $\log C = 14.1$.
Note: The S-N curve is valid for the range $10^5 < N < 10^9$ but extrapolated and applied up to $N = 10^{14}$ due to lack of data.

A one-minute measurement (code ZO40-12, see table 2) was used to calculate the fatigue damage within 20 year lifetime according to Miner's rule:

$$D = \sum \frac{n_i}{N_i}$$

Within 20 years, the one-minute situation is expected to occur $6 \cdot 60 \cdot 365 \cdot 20 = 2.63 \cdot 10^6$ times, assuming an operation of 6 hours a day, 7 days a week.

The loads measured at the pump rod were converted into stresses as follows:

$$S = K_f \cdot \gamma \cdot \frac{F}{\pi \cdot r^2}$$

with K_f representing the stress reserve factor for screw thread which is 1.7 [appendix A] and γ being the safety factor which is 2.0. r is half the diameter of the pump rod. So $S = c \cdot F$ with $c = 67594$, S in (Pa), and F in (N).

The maximum stress range ΔS found in the simulation was 2007 N which corresponds with approximately 135 MPa. As can be seen in Fig. 5.1 of appendix A, this value is very low and indicates that fatigue is not a critical failure criterion. Completed fatigue calculations resulted into $D = 1.47 \cdot 10^{-4}$ which is very small. To check the robustness of the calculations, the Stress Reserve Factor (SRF) was calculated too. The SRF is the factor with which all loads should be multiplied to obtain a fatigue damage of 1. The SRF was found to be 2.7.